Table 1 Relationship between claudin-18 expression and clinicopathologic parameters in 569 CRC cases

	Claudin-18 expression		
	Positive	Negative	*P* value*
Age			
≤65 years	9 (3%)	263	NS
>65 years	12 (4%)	285	
Sex			
Male	10 (3%)	295	NS
Female	11 (4%)	253	
Tumor location			
Right/transverse	8 (4%)	190	NS
Left/sigmoid/rectum	13 (4%)	358	
T grade†			
Tis/T1/T2	7 (5%)	135	NS
T3/T4	14 (3%)	413	
N grade†			
N0	14 (4%)	344	NS
N1/2	7 (3%)	204	
M grade†			
M0	20 (4%)	518	NS
M1	1 (3%)	30	
Stage†			
0/I/II	14 (4%)	335	NS
III/IV	7 (3%)	213	
Histologic type‡			
Well/moderately	19 (3%)	535	NS
Poorly/mucinous	2 (13%)	13	

*Fisher's exact test.

†Tumor stage was classified according to the criteria of the International Union Against Cancer TNM classification of malignant tumors.

‡Histology was according to the World Health Organization (WHO) classification.

CRC, colorectal cancer; NS, not significant.

Table 2 Relationship between claudin-18 expression and various markers in CRC cases

	Claudin-18 expression		
	Positive	Negative	*P* value*
MUC5AC (569)			
Positive	13 (15%)	73	<0.0001
Negative	8 (2%)	475	
MUC6 (569)			
Positive	2 (18%)	9	NS
Negative	19 (3%)	539	
MUC2 (569)			
Positive	18 (5%)	352	NS
Negative	3 (2%)	196	
CD10 (569)			
Positive	4 (2%)	196	NS
Negative	17 (5%)	352	
CDX2 (569)			
Positive	10 (2%)	438	0.0013
Negative	11 (9%)	110	
Claudin-3 (569)			
Reduced	7 (3%)	213	NS
Preserved	14 (4%)	335	
Claudin-4 (569)			
Reduced	10 (3%)	283	NS
Preserved	11 (4%)	265	
Ki-67 (63)			
>50%	7 (37%)	12	NS
0–50%	14 (32%)	30	
p53 (63)			
Positive	12 (32%)	25	NS
Negative	9 (35%)	17	

*Fisher's exact test.

CDX2, caudal-related homeobox gene 2; CRC, colorectal cancer; NS, not significant.

claudin-18, which shows orthotopic expression in normal stomach, might lead to poor survival. In the meantime, ectopic expression of claudin-18 in CRC may affect permeability at tight junctions, possibly increasing the diffusion of nutrients and other extracellular growth factors to promote cancer cell growth, survival and motility. There was no significant correlation between frequency of claudin-18 expression and histological type, but poorly differentiated adenocarcinomas also expressed claudin-18. These results indicated that claudin-18 in CRC contributed to tumor promotion rather than simply worked as cell adhesion. It was recently reported that expression of claudin-18 in patients with UC was significantly upregulated as compared to healthy individuals.[9] Ulcerative colitis is associated with an increased risk of developing CRC.[36] In the present study, non-neoplastic colorectal mucosa and adenoma of the colon did not express claudin-18. There was no clear relationship between expression of claudin-18, Ki-67 and p53. Therefore, we speculated that ectopic expression of claudin-18 in the colon might be associated with invasion in tumor progression, but further analyses are required.

We previously revealed that down-regulation of claudin-18 was preferentially observed in gastric cancer with intestinal phenotype.[7] Recently, Yano *et al.* reported that transcriptional activation of the human claudin-18 gene promoter was regulated through activator protein-1 in phorbol 12-myristate 13-acetate treatment of MKN45 gastric cancer cells,[37] which have gastric phenotype.[38] To date, CRC with gastric phenotype has been reported to frequently exhibit lymphatic permeation and lymph node metastasis.[39] Furthermore, MUC5AC expression was reported to be associated with poor prognosis.[23] These are concordant with the present result. However, the biological interaction between claudin-18 and MUC5AC is poorly understood. In addition, it remains unknown why CRC with expression of MUC5AC has poor prognosis. The previous study has shown very low levels of MUC5AC in normal colon,[40] but abnormal expression of MUC5AC during the early stages of colorectal carcinogenesis has been confirmed by several groups using biochemical, immunohistochemical and molecular biology techniques.[40–43]

CDX2 is reported to be involved in colorectal carcinogenesis[44] as well as the status of its differentiation,[45] and is

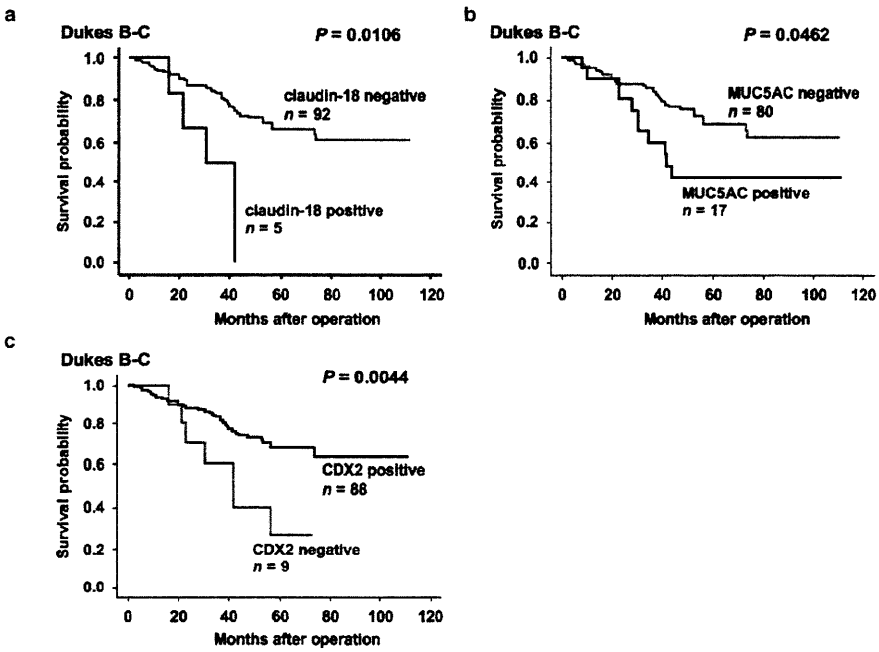

Figure 2 Prognostic value of claudin-18, MUC5AC and CDX2 staining in 97 patients with advanced colorectal cancer (CRC) (Dukes B-C). (**a**) Kaplan–Meier curves of patients with claudin-18-negative or claudin-18-positive CRC. The survival of patients with claudin-18-positive CRC was significantly worse (P = 0.0106, log-rank test). (**b**) MUC5AC-negative or MUC5AC-positive CRC. The survival of patients with MUC5AC-positive CRC was significantly worse (P = 0.0462, log-rank test). (**c**) CDX2-negative or CDX2-positive CRC. The survival of patients with CDX2-negative CRC was significantly worse (P = 0.0044, log-rank test).

Table 3 Multivariate analysis of factors influencing survival in 117 CRC cases

Factor	Hazard ratio	95% CI	χ^2	P value
Age				
≤65 years	1	Reference	1.356	NS
>65 years	1.46	0.772–2.761		
Sex				
Female	1	Reference	0.307	NS
Male	1.204	0.625–2.321		
Tumor location				
Right/transverse	1	Reference	0.694	NS
Left/sigmoid/rectum	1.476	0.591–3.689		
T grade†				
Tis/T1/T2	1	Reference	6.565	0.0104
T3/T4	4.999	1.459–17.122		
N grade†				
N0	1	Reference	2.661	NS
N1/2	5.5	0.709–42.625		
M grade†				
M0	1	Reference	4.97	0.0258
M1	2.311	1.106–4.282		
Stage†				
0/I/II	1	Reference	0.062	NS
III/IV	1.326	0.145–12.16		
Histologic type‡				
Well/moderately	1	Reference	1.73	NS
Poorly/mucinous	4.157	0.497–34.738		
Claudin-18				
Negative	1	Reference	5.331	0.0209
Positive	3.603	1.214–10.695		

†Tumor stage was classified according to the criteria of the International Union against Cancer TNM classification of malignant tumors.

‡Histology was according to the World Health Organization (WHO) classification.

NS, not significant.

known to be a tumor suppressor.[46] Down-regulation of CDX2 in CRC was reported to increase throughout tumor progression,[25,46] and expression of CDX2 was reported to reduce the tumorigenesis in CRC cell lines.[47] In the present study, the prognosis of patients with negative CDX2 expression was significantly poorer than patients with positive expression. To date, little is known about the relationship between claudin-18 and CDX2 expression, but Satake *et al.* reported that expression of claudin-18 was not altered by ectopic CDX2 in gastric cancer cell lines.[48] In the present study, positive expression of claudin-18 showed significant correlation with positive expression of MUC5AC and negative expression of CDX2. There might be no direct association between claudin-18, MUC5AC and CDX2. Double-immunohistochemical staining, however, showed coexpression of claudin-18 with MUC5AC in many tumor cells, and these molecules might be controlled by common transcription factors. SOX2 is an HMG-box transcription factor expressed in gastric mucosa but not in intestine. Park *et al.* reported that aberrant expression of SOX2 up-regulated MUC5AC in CRC.[49] In addition, Tsukamoto *et al.* reported that the immunohistochemical expression patterns of SOX2 and CDX2 were inversely related in the human stomach.[50] Further studies should be performed in the near future to elucidate a role for SOX2 in regulation of claudin-18 in CRC.

Morphological analysis revealed that CRC with both claudin-18 and MUC5AC expression are more likely to resemble gastric tubular adenocarcinoma in appearance than CRC with MUC5AC expression alone. Both claudin-18 and MUC5AC show orthotopic expression in normal stomach, and their ectopic expression in CRC may lead to

morphological resemblance to gastric cancer. Colorectal cancer with gastric phenotype is closely associated with specific genetic subtypes, such as microsatellite instability (MSI). CDX2 was also reported to be mutated in CRC with microsatellite instability-high (MSI-H).[51] Colorectal cancer with both claudin-18 and MUC5AC expression in the present study had few typical clinicopathological features of CRC with MSI-H (poorly differentiated or mucinous appearance, often with prominent tumor-infiltrating lymphocytes, and tendency for right side), but further examinations are required.

Indeed TMAs cannot be used to evaluate the heterogeneous expression patterns of various cancer-related molecules, but we examined 569 CRC cases that included 174 samples from surgically resected specimens. Furthermore, use of TMAs to immunophenotype malignant tumors was previously validated by Hoos *et al.* [52] and their data showed an excellent concordance between the results obtained when TMAs were used with triplicate cores per tumor and with full sections. In summary, we revealed that CRC with claudin-18 expression has a poor prognosis and demonstrates a gastric phenotype that is significantly MUC5AC-positive or CDX2-negative in expression. Claudin-18 may be a useful marker to predict CRC with poor prognosis.

ACKNOWLEDGMENTS

We thank Ms. Emiko Hisamoto and Mr Shinichi Norimura for excellent technical assistance and advice. This work was carried out with the kind cooperation of the Research Center for Molecular Medicine, Faculty of Medicine, Hiroshima University. We thank the Analysis Center of Life Science, Hiroshima University, for the use of their facilities. This work was supported, in part, by Grants-in-Aid for Cancer Research from the Ministry of Education, Culture, Science, Sports and Technology of Japan; in part by a Grant-in-Aid for the Third Comprehensive 10-Year Strategy for Cancer Control and for Cancer Research from the Ministry of Health, Labour and Welfare of Japan.

REFERENCES

1 Jemal A, Siegel R, Ward E *et al.* Cancer statistics, 2008. *CA Cancer J Clin* 2008; **58**: 71–96.
2 Gumbiner BM. Carcinogenesis: A balance between beta-catenin and APC. *Curr Biol* 1997; **7**: 443–6.
3 Kuwai T, Kitadai Y, Tanaka S *et al.* Single nucleotide polymorphism in the hypoxia-inducible factor-1alpha gene in colorectal carcinoma. *Oncol Rep* 2004; **12**: 1033–7.
4 Oue N, Kuniyasu H, Noguchi T *et al.* Serum concentration of Reg IV in patients with colorectal cancer: Overexpression and high serum levels of Reg IV are associated with liver metastasis. *Oncology* 2007; **72**: 371–80.
5 Tsukita S, Furuse M, Itoh M. Multifunctional strands in tight junctions. *Nat Rev Mol Cell Biol* 2001; **2**: 285–93.
6 Niimi T, Nagashima K, Ward JM *et al.* claudin-18, a novel downstream target gene for the T/EBP/NKX2.1 homeodomain transcription factor, encodes lung- and stomach-specific isoforms through alternative splicing. *Mol Cell Biol* 2001; **21**: 7380–90.
7 Sanada Y, Oue N, Mitani Y, Yoshida K, Nakayama H, Yasui W. Down-regulation of the claudin-18 gene, identified through serial analysis of gene expression data analysis, in gastric cancer with an intestinal phenotype. *J Pathol* 2006; **208**: 633–42.
8 Sahin U, Koslowski M, Dhaene K *et al.* Claudin-18 splice variant 2 is a pan-cancer target suitable for therapeutic antibody development. *Clin Cancer Res* 2008; **14**: 7624–34.
9 Zwiers A, Fuss IJ, Leijen S, Mulder CJ, Kraal G, Bouma G. Increased expression of the tight junction molecule claudin-18 A1 in both experimental colitis and ulcerative colitis. *Inflamm Bowel Dis* 2008; **14**: 1652–9.
10 Sentani K, Oue N, Tashiro T *et al.* Immunohistochemical staining of Reg IV and claudin-18 is useful in the diagnosis of gastrointestinal signet ring cell carcinoma. *Am J Surg Pathol* 2008; **32**: 1182–9.
11 Mees ST, Mennigen R, Spieker T *et al.* Expression of tight and adherens junction proteins in ulcerative colitis associated colorectal carcinoma: Upregulation of claudin-1, claudin-3, claudin-4, and beta-catenin. *Int J Colorectal Dis* 2009; **24**: 361–8.
12 Ueda J, Semba S, Chiba H *et al.* Heterogeneous expression of claudin-4 in human colorectal cancer: Decreased claudin-4 expression at the invasive front correlates cancer invasion and metastasis. *Pathobiology* 2007; **74**: 32–41.
13 Matsuda Y, Semba S, Ueda J *et al.* Gastric and intestinal claudin expression at the invasive front of gastric carcinoma. *Cancer Sci* 2007; **98**: 1014–9.
14 Kim YS, Gum J Jr, Brockhausen I. Mucin glycoproteins in neoplasia. *Glycoconj J* 1996; **13**: 693–707.
15 Tatematsu M, Ichinose M, Miki K, Hasegawa R, Kato T, Ito N. Gastric and intestinal phenotypic expression of human stomach cancers as revealed by pepsinogen immunohistochemistry and mucin histochemistry. *Acta Pathol Jpn* 1990; **40**: 494–504.
16 Yoshikawa A, Inada Ki K, Yamachika T, Shimizu N, Kaminishi M, Tatematsu M. Phenotypic shift in human differentiated gastric cancers from gastric to intestinal epithelial cell type during disease progression. *Gastric Cancer* 1998; **1**: 134–41.
17 Tajima Y, Yamazaki K, Nishino N *et al.* Gastric and intestinal phenotypic marker expression in gastric carcinomas and recurrence pattern after surgery-immunohistochemical analysis of 213 lesions. *Br J Cancer* 2004; **91**: 1342–8.
18 Hollingsworth MA, Swanson BJ. Mucins in cancer: Protection and control of the cell surface. *Nat Rev Cancer* 2004; **4**: 45–60.
19 Byrd JC, Bresalier RS. Mucins and mucin binding proteins in colorectal cancer. *Cancer Metastasis Rev* 2004; **23**: 77–99.
20 Eaden JA, Abrams KR, Mayberry JF. The risk of colorectal cancer in ulcerative colitis: A meta-analysis. *Gut* 2001; **48**: 526–35.
21 Tatsumi N, Kushima R, Vieth M *et al.* Cytokeratin 7/20 and mucin core protein expression in ulcerative colitis-associated colorectal neoplasms. *Virchows Arch* 2006; **448**: 756–62.
22 Femia AP, Tarquini E, Salvadori M *et al.* K-ras mutations and mucin profile in preneoplastic lesions and colon tumors induced in rats by 1,2-dimethylhydrazine. *Int J Cancer* 2008; **122**: 117–23.
23 Kocer B, McKolanis J, Soran A. Humoral immune response to MUC5AC in patients with colorectal polyps and colorectal carcinoma. *BMC Gastroenterol* 2006; **6**: 4.
24 Chawengsaksophak K, James R, Hammond VE, Kontgen F, Beck F. Homeosis and intestinal tumours in Cdx2 mutant mice. *Nature* 1997; **386**: 84–7.

25 Kaimaktchiev V, Terracciano L, Tornillo L *et al.* The homeobox intestinal differentiation factor CDX2 is selectively expressed in gastrointestinal adenocarcinomas. *Mod Pathol* 2004; **17**: 1392–9.
26 Hamilton SR, Aaltonen LA, eds. *World Health Organization Classification of Tumours. Pathology and Genetics of Tumours of the Digestive System.* Lyon: IARC Press, 2000.
27 Sobin LH, Wittekind CH, eds. *TNM Classification of Malignant Tumors*, 6th edn. New York: John Wiley & Sons, 2002; 65–8.
28 Mizoshita T, Tsukamoto T, Nakanishi H *et al.* Expression of Cdx2 and the phenotype of advanced gastric cancers: Relationship with prognosis. *J Cancer Res Clin Oncol* 2003; **129**: 727–34.
29 Oue N, Mitani Y, Aung PP *et al.* Expression and localization of Reg IV in human neoplastic and non-neoplastic tissues: Reg IV expression is associated with intestinal and neuroendocrine differentiation in gastric adenocarcinoma. *J Pathol* 2005; **207**: 185–98.
30 Mantel N. Evaluation of survival data and two new rank order statistics arising in its consideration. *Cancer Chemother Rep* 1966; **50**: 163–70.
31 Hough CD, Sherman-Baust CA, Pizer ES *et al.* Large-scale serial analysis of gene expression reveals genes differentially expressed in ovarian cancer. *Cancer Res* 2000; **60**: 6281–7.
32 Agarwal R, D'Souza T, Morin PJ. Claudin-3 and claudin-4 expression in ovarian epithelial cells enhances invasion and is associated with increased matrix metalloproteinase-2 activity. *Cancer Res* 2005; **65**: 7378–85.
33 Hoevel T, Macek R, Swisshelm K, Kubbies M. Reexpression of the TJ protein CLDN1 induces apoptosis in breast tumor spheroids. *Int J Cancer* 2004; **108**: 374–83.
34 Michl P, Barth C, Buchholz M *et al.* Claudin-4 expression decreases invasiveness and metastatic potential of pancreatic cancer. *Cancer Res* 2003; **63**: 6265–71.
35 Hewitt KJ, Agarwal R, Morin PJ. The claudin gene family: Expression in normal and neoplastic tissues. *BMC Cancer* 2006; **6**: 186.
36 Itzkowitz SH, Present DH. Consensus conference: Colorectal cancer screening and surveillance in inflammatory bowel disease. *Inflamm Bowel Dis* 2005; **11**: 314–21.
37 Yano K, Imaeda T, Niimi T. Transcriptional activation of the human claudin-18 gene promoter through two AP-1 motifs in PMA-stimulated MKN45 gastric cancer cells. *Am J Physiol Gastrointest Liver Physiol* 2008; **294**: 336–43.
38 Matsuda K, Yamauchi K, Matsumoto T, Sano K, Yamaoka Y, Ota H. Quantitative analysis of the effect of Helicobacter pylori on the expressions of SOX2, CDX2, MUC2, MUC5AC, MUC6, TFF1, TFF2, and TFF3 mRNAs in human gastric carcinoma cells. *Scand J Gastroenterol* 2008; **43**: 25–33.
39 Yao T, Tsutsumi S, Akaiwa Y *et al.* Phenotypic expression of colorectal adenocarcinomas with reference to tumor development and biological behavior. *Jpn J Cancer Res* 2001; **92**: 755–61.
40 Biemer-Huttmann AE, Walsh MD, McGuckin MA *et al.* Immunohistochemical staining patterns of MUC1, MUC2, MUC4, and MUC5AC mucins in hyperplastic polyps, serrated adenomas, and traditional adenomas of the colorectum. *J Histochem Cytochem* 1999; **47**: 1039–48.
41 Buisine MP, Janin A, Maunoury V *et al.* Aberrant expression of a human mucin gene (MUC5AC) in rectosigmoid villous adenoma. *Gastroenterology* 1996; **110**: 84–91.
42 Bartman AE, Sanderson SJ, Ewing SL *et al.* Aberrant expression of MUC5AC and MUC6 gastric mucin genes in colorectal polyps. *Int J Cancer* 1999; **80**: 210–18.
43 Myerscough N, Sylvester PA, Warren BF *et al.* Abnormal subcellular distribution of mature MUC2 and de novo MUC5AC mucins in adenomas of the rectum: Immunohistochemical detection using non-VNTR antibodies to MUC2 and MUC5AC peptide. *Glycoconj J* 2001; **18**: 907–14.
44 Mallo GV, Rechreche H, Frigerio JM *et al.* Molecular cloning, sequencing and expression of the mRNA encoding human Cdx1 and Cdx2 homeobox. Down-regulation of Cdx1 and Cdx2 mRNA expression during colorectal carcinogenesis. *Int J Cancer* 1997; **74**: 35–44.
45 Hinoi T, Tani M, Lucas PC *et al.* Loss of CDX2 expression and microsatellite instability are prominent features of large cell minimally differentiated carcinomas of the colon. *Am J Pathol* 2001; **159**: 2239–48.
46 Bonhomme C, Duluc I, Martin E *et al.* The Cdx2 homeobox gene has a tumour suppressor function in the distal colon in addition to a homeotic role during gut development. *Gut* 2003; **52**: 1465–71.
47 Hinoi T, Loda M, Fearon ER. Silencing of CDX2 expression in colon cancer via a dominant repression pathway. *J Biol Chem* 2003; **278**: 44608–16.
48 Satake S, Semba S, Matsuda Y *et al.* Cdx2 transcription factor regulates claudin-3 and claudin-4 expression during intestinal differentiation of gastric carcinoma. *Pathol Int* 2008; **58**: 156–63.
49 Park ET, Gum JR, Kakar S, Kwon SW, Deng G, Kim YS. Aberrant expression of SOX2 upregulates MUC5AC gastric foveolar mucin in mucinous cancers of the colorectum and related lesions. *Int J Cancer* 2008; **122**: 1253–60.
50 Tsukamoto T, Inada K, Tanaka H *et al.* Down-regulation of a gastric transcription factor, Sox2, and ectopic expression of intestinal homeobox genes, Cdx1 and Cdx2: Inverse correlation during progression from gastric/intestinal-mixed to complete intestinal metaplasia. *J Cancer Res Clin Oncol* 2004; **130**: 135–45.
51 Jass JR. Classification of colorectal cancer based on correlation of clinical, morphological and molecular features. *Histopathology* 2007; **50**: 113–30.
52 Hoos A, Urist MJ, Stojadinovic A *et al.* Validation of tissue microarrays for immunohistochemical profiling of cancer specimens using the example of human fibroblastic tumors. *Am J Pathol* 2001; **158**: 1245–51.

Potential role for vascular endothelial growth factor-D as an autocrine factor for human gastric carcinoma cells

Miwako Tanaka,[1] Yasuhiko Kitadai,[1,4] Michiyo Kodama,[1] Kei Shinagawa,[1] Tomonori Sumida,[1] Shinji Tanaka,[2] Naohide Oue,[3] Wataru Yasui[3] and Kazuaki Chayama[1]

[1]Department of Medicine and Molecular Science, Hiroshima University Graduate School of Biomedical Sciences, Hiroshima; [2]Department of Endoscopy, Hiroshima University Hospital, Hiroshima; [3]Molecular Pathology, Hiroshima University Graduate School of Biomedical Sciences, Hiroshima, Japan

(Received April 5, 2010/Revised June 1, 2010/Accepted June 12, 2010/Accepted manuscript online June 17, 2010/Article first published online July 6, 2010)

Vascular endothelial growth factor (VEGF)-D induces lymphangiogenesis by activating VEGF receptor (VEGFR)-3, which is expressed mainly by lymphatic endothelial cells. VEGFR-3 has also been detected in several types of malignant cells, but the significance of VEGFR-3 expression by malignant cells remains unclear. We examined the expression and function of VEGF-D/VEGFR-3 in human gastric carcinoma cells. Expression of VEGF-D and VEGFR-3 was analyzed in three human gastric carcinoma cell lines and 29 surgical specimens. cDNA microarray analysis was used to examine the effect of VEGF-D on the expression of genes associated with disease progression in VEGFR-3-expressing KKLS cells. VEGF-D-transfected cells and control cells were transplanted into the gastric wall of nude mice. In 10 of the 29 (34%) gastric carcinoma specimens and two of the three cell lines, cancer cells expressed both VEGF-D and VEGFR-3. *In vitro* treatment of KKLS cells with exogenous VEGF-D increased expression of cyclin D1 and Bcl-2 and stimulated cell proliferation. VEGF-D transfection into KKLS cells resulted in stimulation of angiogenesis, lymphangiogenesis, and cell proliferation, and in inhibition of apoptosis. VEGF-D may participate in the progression of human gastric carcinoma by acting via autocrine and paracrine mechanisms. (*Cancer Sci* 2010; 101: 2121–2127)

Gastric cancer is one of the most frequently occurring malignancies in the world.[1] Acquisition of metastatic potential by tumor cells results in a poor prognosis for patients with gastric carcinoma. The extent of lymph node metastasis is one of the most important prognostic factors and determines the course of cancer therapy.[2]

Lymphangiogenesis and angiogenesis are regulated by members of the vascular endothelial growth factor (VEGF) family and their receptors.[3,4] VEGF-A is a major inducer of angiogenesis and vessel permeability.[5,6] The VEGF family includes VEGF-A, -B, -C, -D, -E, -F, and placental growth factor (PlGF).[7] VEGF-D, also known as c-fos-induced growth factor,[8] is secreted as a preprotein that undergoes proteolytic processing.[9] Full-length VEGF-D displays high affinity for VEGFR-3, whereas its affinity for VEGFR-2 is increased through progressive proteolytic cleavage.[9] In animal studies, VEGF-D has been shown to enhance tumor angiogenesis and lymphangiogenesis, thereby promoting metastatic spread of tumor cells via the lymphatics.[10–12] In clinical studies, correlation between expression of VEGF-D by tumor cells and lymph node metastasis has been reported.[13–18] In contrast, some clinical studies have shown that the level of VEGF-D expression is lower in tumor tissue than in the corresponding normal tissue.[19–23] Therefore, it remains controversial whether VEGF-D is the main regulator of lymphangiogenesis. Because of its structural similarity to VEGF-C, VEGF-D is thought to have a similar biologic effect. Recently, we studied the expression and role of the VEGF-C/VEGFR-3 axis in human gastric carcinoma.[24] We showed that the tumor cells expressed not only VEGF-C but also VEGFR-3. *In vitro and in vivo* experiments showed that VEGF-C acts as a progressive growth factor, in addition to acting as a lymphangiogenic and angiogenic factor. However, the autocrine role of VEGF-D in gastric carcinoma cells has not been characterized. Thus, we analyzed the role of the VEGF-D/VEGFR-3 axis in human gastric carcinoma cells.

Materials and Methods

Surgical specimens of gastric carcinoma. Paraffin-embedded archival specimens of invasive gastric carcinoma obtained from 29 patients who underwent surgical resection at Hiroshima University Hospital were studied by immunohistochemistry. All tumors had invaded beyond the submucosa. The criteria for staging and histologic classification were those proposed by the Japanese Research Society for Gastric Cancer.[25] The patient group comprised 27 men and two women, with a median age of 66 years (range, 34–81 years). The tissues were immediately snap-frozen and stored in liquid nitrogen for semiquantitative RT-PCR.

Cell cultures. Three cell lines established from human gastric carcinomas were maintained in RPMI-1640 medium (Nissui, Tokyo, Japan) with 10% FBS (MA BioProducts, Walkersville, MD, USA). The TMK-1 cell line (derived from poorly differentiated adenocarcinoma) was provided by Dr E. Tahara (Hiroshima University, Hiroshima, Japan). The KKLS cell line (derived from undifferentiated carcinoma) was provided by Dr Y. Takahashi (Chiba University, Chiba, Japan). The MKN-1 cell line (derived from adenosquamous carcinoma) was obtained from the Health Science Research Resources Bank (Osaka, Japan).

Cell proliferation assay. *In vitro* growth was measured with a Cell Proliferation Biotrak ELISA System, version 2 (Amersham Biosciences, Piscataway, NJ, USA) according to the manufacturer's instructions to determine whether recombinant human VEGF-D (rhVEGF-D) (R&D Systems, Minneapolis, MN, USA) would stimulate proliferation of KKLS cells and TMK-1 cells. Cells (1×10^4) were seeded on a 96-well plate, and BrdU (final concentration, 10 μM) was added to the culture medium with or without rhVEGF-D (2, 20, or 100 ng/mL) for 24 h. Cell proliferation was quantified in a plate reader (Microplate Manager 5.2.1; Bio-Rad, Hercules, CA, USA) at 450 nm.

[4]To whom correspondence should be addressed.
E-mail: kitadai@hiroshima-u.ac.jp

doi: 10.1111/j.1349-7006.2010.01649.x

Microarray analysis. We performed microarray analysis using the Human Cancer CHIP (version 4; Takara Shuzo, Kyoto, Japan), in which 886 human cancer-related genes are spotted on glass plates. KKLS cells were cultured in RPMI-1640 medium without FBS for 6 h and then cultured with or without rhVEGF-D (20 ng/mL) for 8 h. A fluorescent probe synthesized by reverse transcription of 1 μg of the mRNA with 50 U AMV reverse transcriptase (Takara Shuzo) was added to each reaction mixture. Cy3- and Cy5-labeled probes were prepared by using mRNAs isolated from control cells and rhVEGF-D cells, and both were mixed in the reaction buffer (6× SSC/0.2% SDS and 5× Denhardt's solution, 0.8 mg/mL poly [dA], and 1 mg/mL yeast tRNA). The mixture was hybridized to the cDNA CHIP at 65°C overnight. The CHIP was washed twice with 2× SSC/0.2% SDS solution at 55°C for 30 min and then with the same solution at 65°C for 5 min. Finally, the CHIP was washed with 0.05 × SSC at room temperature for 10 min. Signals on the hybridized CHIP were visualized and quantified with a ScanArray 5000 laser scanner (GSI Lomonids) and normalized to the averaged signals of housekeeping genes. Genes were excluded from further investigation when the intensities of both Cy3 and Cy5 were below 1000 fluorescence units. Those with Cy3/Cy5 signal ratios >2.0 were regarded as up-regulated.

Semiquantitative reverse transcription-polymerase chain reaction (RT-PCR) and quantitative real-time PCR. Total RNA was extracted from the gastric cancer cell lines with an RNeasy Kit (Qiagen, Tokyo, Japan) according to the manufacturer's instructions. RT-PCR was performed with the isolated RNA (1 μg). cDNA was generated from 1 μg of total RNA with a First-Strand cDNA Synthesis Kit (Amersham Biosciences, Buckinghamshire, UK). The primers and annealing temperatures for VEGF-D, VEGFR-2, VEGFR-3, β-actin, GAPDH, and Bcl-2 are given in Table 1. The primers were designed with specific Primer analysis software (Primer Designer; Scientific and Educational Software, Arlington, MA, USA), and the specificities of the sequences were confirmed by FASTA analysis (EMBL Nucleotide Sequence Database). Semiquantitative RT-PCR was performed with an AmpliTaq Gold Kit (Roche, Mannheim, Germany), and quantitative real-time PCR was performed with a LightCycler-FastStart DNA Master SYBR-Green I Kit (Roche) according to the manufacturer's instructions. Quantitative real-time PCR was used to monitor gene expression and was performed with a LightCycler system and Light Cycler Data Analysis Software version 3.5 (Roche) according to standard procedures. To correct for differences in both RNA quality and quantity between samples, the data were normalized to those for β-actin.

Immunofluorescence staining for pVEGFR-3. KKLS cells were cultured in RPMI-1640 medium without FBS for 24 h, then treated with or without rhVEGF-D (20 ng/mL) for 10 min. pVEGFR-2,3 (1:1000; Calbiochem, San Diego, CA, USA) was used to stain pVEGFR-2,3 in tumor cells.

Western blot analysis. Western blotting was used to evaluate the expression of cyclin D1, Akt and MAPK, p38, and JNK phosphorylation. To evaluate Akt, MAPK, p38, and JNK phosphorylation of KKLS cells, cells were plated at 1.5×10^5 cells/mL per well in a six-well plate and incubated overnight. Cells were then starved for 24 h in serum-free medium and stimulated with rhVEGF-D (20 ng/mL) or rhVEGF-C (20 ng/mL) (R&D Systems) for 10 min at 37°C. After stimulation, cells were washed three times in cold PBS containing 1 mmol/L sodium. Cell lysates were prepared with M-PER Mammalian Protein Extraction Reagent (Pierce, Rockford, IL, USA). Samples of cell lysates (20 μg protein) were separated by SDS-PAGE and transferred to nitrocellulose transfer membranes (Whatman, Dassel, Germany). Blots were blocked for 1 h at room temperature in TBS containing 1% skim milk and 0.1% Tween 20. Membranes were incubated overnight at 4°C with primary antibodies against polyclonal mouse antihuman cyclin D1 (Dako, Glostrup, Denmark), polyclonal rabbit antibody to phospho-Akt (phosphorylated at Ser473; Cell Signaling Technology, Beverly, MA, USA), phospho-MAPK, p38, JNK (Promega, Madison, WI, USA), and β-actin (Sigma, St. Louis, MO, USA). Membranes were then washed three times in TBS containing 0.1% Tween 20 and incubated with secondary antibody for 1 h at room temperature. Immune complexes were visualized by enhanced chemiluminescence with an ECL Plus Kit (Amersham Biosciences).

Gene transfection and cloning of transfected cell lines. Full-length human VEGF-D cDNA was inserted into the EcoRI-EcoRI site of pBR322 (Invitrogen, Carlsbad, CA, USA). The resultant plasmid was digested with XbaI-BamHI and cloned into the XbaI-BamHI site of the pcDNA4/myc-His vector (Invitrogen) to yield VEGF-D expression. Expression of VEGF-D cDNA was under the control of the cytomegalovirus promoter. KKLS cells were transfected with either the full-length VEGF-D cDNA or empty pcDNA4/myc-His vector by using Lipofectin (Life Technologies, Gaithersburg, MD, USA) according to the manufacturer's instructions. After transfection, cells were grown in selective medium (10% FBS-RPMI-1640 containing 400 μg/mL Zeocin). Zeocin-resistant colonies were lifted from culture dishes and grown individually to establish stable VEGF-D-overexpressing clonal lines.

Enzyme-linked immunosorbent assay (ELISA) for VEGF-D protein. KKLS cells were plated at 1.5×10^5 cells/mL per well

Table 1. Application of PCR

Gene	Primer sequences	Number of cycles	Annealing temperature	Product size (bp)
VEGF-D	F: 5′-GTATGGACTCTCGCTCAGCAT-3′ R: 5′-AGGCTCTCTTCATTGCAACAG-3′	32	59	226
VEGFR-2	F: 5′-GCATCTCATCTGTTACAGC-3′ R: 5′-CTTCATCAATCTTTACCCC-3′	32	62	331
VEGFR-3	F: 5′-GGTTCCTCCAGGATGAAGAC-3′ R: 5′-CAAGCAGTAACGCCAGTGTC-3′	32	62	505
β-Actin	F: 5′-GGACTTCGAGCAAGAGATGG-3′ R: 5′-AGCACTGTGTTGGCGTACAG-3′	35	55	234
GAPDH	F: 5′-ATCATCCCTGCCTCTACTGG-3′ R: 5′-CCCTCCGACGCCTGCTTCAC-3′	28	55	188
Bcl-2	F: 5′-GGTGGAGGAGCTCTTCCAGG-3′ R: 5′-ACAGTTCCACAAAGGCATCC-3′	35	60	206

VEGF-D, vascular endothelial growth factor D; VEGFR-2, VEGF receptor 2.

doi: 10.1111/j.1349-7006.2010.01649.x

in a six-well plate (Becton Dickinson Labware, Franklin Lakes, NJ, USA) and cultured in RPMI-1640 containing 10% FBS. After 48 h, the supernatants were collected and used to measure VEGF-D protein. We used the Quantikine Human VEGF-D Immunoassay (R&D Systems) according to the manufacturer's instructions to measure VEGF-D levels.

***In vitro* cell growth.** Cells (1×10^4) were seeded in a six-well plate and cultured in RPMI-1640 containing 0.5% FBS. The medium was changed every 48 h. Cell counts were determined with a Countess Automated Cell Counter (Invitrogen) from triplicate cultures.

Animal models. Male athymic BALB/c nude mice were obtained from Charles River Japan (Tokyo, Japan). The mice were maintained under specific pathogen-free conditions and used when 5 weeks old. Experiments were done according to the animal experimental guidelines of Hiroshima University.

Orthotopic (gastric mucosa) xenograft model. To produce gastric tumors, KKLS/VEGF-D and KKLS/control cells growing in culture were harvested from subconfluent cultures by brief treatment with 0.25% trypsin and 0.02% EDTA. Cells (1×10^6) were resuspended in HANKS and implanted into the gastric wall of nude mice under a zoom stereo microscope. After 4 weeks, the mice were killed and tumors were resected for study.

Immunohistochemistry. Formalin-fixed, paraffin-embedded serial sections (4 μm) were deparaffinized and rehydrated. Sections were immunostained for VEGF-D, VEGFR-3, Ki-67, and Lyve1. Antigen retrieval was performed in Dako REAL Target Retrieval Solution (Dako) in a microwave oven for 10 min. Endogenous peroxidase activity was blocked with 3% hydrogen peroxide in 100% methanol for 10 min. Sections were washed with PBS and blocked with 3% normal horse serum for 10 min. Frozen sections (8 μm) were immunostained for CD31 and fixed in cold acetone for 10 min. VEGF-D was detected with goat antihuman polyclonal antibody (1:200; R&D Systems), and VEGFR-3 was detected with goat antihuman polyclonal antibody (1:50; R&D Systems). Ki-67 was detected with mouse antihuman polyclonal antibody (MIB-1, 1:25; Dako), and Lyve1 was detected with rat antimouse monoclonal antibody (1:20; R&D Systems). CD31 was detected with rat antimouse polyclonal antibody (1:200; Pharmingen, San Diego, CA, USA). Sections were incubated overnight at 4°C with the primary antibodies. Sections were then washed with PBS three times and incubated for 1 h with peroxidase-conjugated secondary antibody. A positive reaction was detected by exposure to stable 3,3′-diaminobenzidine. The slides were counterstained with hematoxylin.

Quantification of Ki-67 labeling index, lymphatic vessel density (LVD), and Microvessel density (MVD). MVD was determined from the counts of CD31-positive vessels. Vessel density was assessed by light microscopy of the intratumoral and peritumoral lesions containing the greatest number of capillaries and small venules. Highly vascular areas were identified by scanning tumor sections at low power (×40 and ×100). After the six areas of greatest neovascularization were identified, a vessel count was performed at ×400, and the mean count of six fields was calculated and defined as the mean MVD. Identification of a vessel lumen was not necessary for a structure to be defined as a vessel.[26] Lymphatic activity was evaluated according to the area of lymphatic vessels stained with anti-Lyve1 antibody. For quantification of the lymphatic vessel area, six random fields at ×400 magnification were captured for each tumor, and the outline of each lymphatic vessel including a lumen was manually traced. The area was then calculated with the use of NIH ImageJ software. Ki-67 staining was assessed by determining the Ki-67 labeling index by means of light microscopy at the sites of the greatest number of Ki-67-positive cells. Cells were counted in ten fields at ×40 magnification, and the mean percentage of stained cells was calculated. The mean percentage of Ki-67-positive cells was taken as the Ki-67 labeling index.

Histochemical detection of apoptosis and determination of apoptotic index. Apoptotic cells in tissue sections were detected by terminal deoxynucleotide transferase-mediated TUNEL with the ApopTag Plus Peroxidase *In Situ* Apoptosis Detection Kit (Chemicon, Temecula, CA, USA) according to manufacturer's instructions. The apoptotic index was expressed as the ratio of positively stained tumor cells and bodies to all tumor cells, given as a percentage for each case. Five random fields in a section were selected by light microscopy; at least 1000 cells were counted under ×400 magnification.

Statistical analysis. The chi-squared test was used for analysis of categoric data, and the Mann–Whitney *U*-test was used for analysis of continuous variables. The significance level was set at 5% for all analysis.

Results

Immunohistochemistry for VEGF-D and VEGFR-3 in human gastric carcinoma tissues. We examined expression of VEGF-D and VEGFR-3 protein in 29 human gastric carcinoma tissues by immunohistochemistry. VEGFR-3 expression was observed on lymphatic endothelial cells. Of the 29 specimens of gastric carcinoma, 14 (48%) showed intense VEGF-D immunoreactivity (Fig. 1a,b), and 15 (52%) showed intense VEGFR-3 immunoreactivity (Fig. 1c,d) on tumor cells. In 10 of the 29 (34%) gastric carcinoma specimens, tumor cells expressed both VEGF-D and VEGFR-3. When the VEGF-D expression was analyzed in relation to histological types, positivity for VEGF-D in the diffuse (undifferentiated) type (7/10, 70%) was significantly higher than that in the intestinal (differentiated) type (7/19, 36%).

Expression of VEGF-D, VEGFR-2, VEGFR-3 mRNA in gastric carcinoma cell lines. We examined expression of VEGF-D, VEGFR-2, VEGFR-3 mRNA in gastric cancer cell lines by semiquantitative RT-PCR. All gastric carcinoma cell lines constitutively expressed VEGF-D mRNA. Expression of VEGFR-2 mRNA was not observed in any of the cell lines examined. Two of the three cell lines expressed VEGFR-3 mRNA (Fig. 2a). KKLS cells expressed VEGFR-3 at a high level; therefore, we used KKLS cells for further studies. Treatment of KKLS cells with VEGF-D induced phosphorylation of VEGFR-3 (Fig. 1e,f) and its downstream signaling molecule, Akt (Fig. 2b). Furthermore, treatment of KKLS cells with VEGF-D resulted in stimulation of cell proliferation. Treatment with VEGF-D did not stimulate proliferation of TMK-1 cells (VEGFR-3 negative) (Fig. 2c).

VEGF-D up-regulated expression of several genes associated with disease progression in KKLS cells. To investigate the various cancer-related genes up-regulated by VEGF-D, we performed microarray analysis. Various mRNA expression levels were compared between control KKLS cells and cells treated with rhVEGF-D for 8 h. Microarray analysis revealed up-regulation of 52 genes by VEGF-D stimulation. Representative genes that were up-regulated in cells treated with rhVEGF-D are shown in Table 2. Among these genes, we confirmed increased expression of Bcl-2 by quantitative real-time PCR (Fig. 3a) and of cyclin D1 (Fig. 3b) by western blotting. Treatment with VEGF-D increased expression of Bcl-2 mRNA and cyclin D1 protein.

Establishment of VEGF-D-overexpressing clonal cell line. To examine the biological function of VEGF-D, VEGF-D expression vector or the empty vector was stably transfected into KKLS cells. Overexpression of VEGF-D mRNA and protein was confirmed by quantitative real-time PCR (Fig. 4a) and ELISA (Fig. 4b), respectively.

***In vitro* and *in vivo* proliferation of VEGF-D-transfected KKLS cells.** The effect of overexpression of VEGF-D on the ability of

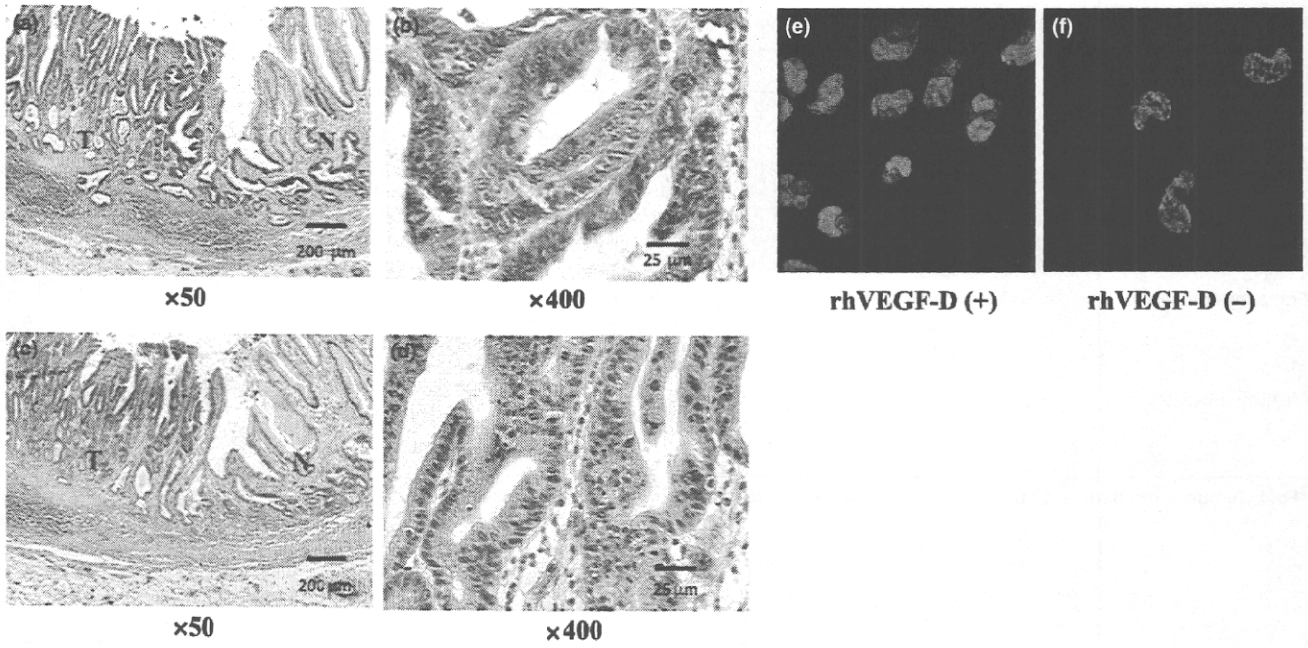

Fig. 1. Immunohistochemical staining for (a,b) VEGF-D and (c,d) VEGFR-3 in human gastric carcinoma tissues. Immunoreactivities for VEGF-D and VEGFR-3 were detected in tumor cells (T) but not in normal gastric mucosa (N). Scale bars: (a,c) 200 μm, (b,d) 25 μm. Immunofluorescence staining for phosphorylation of VEGFR-3 after stimulation with (e) or without (f) VEGF-D in KKLS cells. Tumor cells stained positively for pVEGFR-2,3 (red).

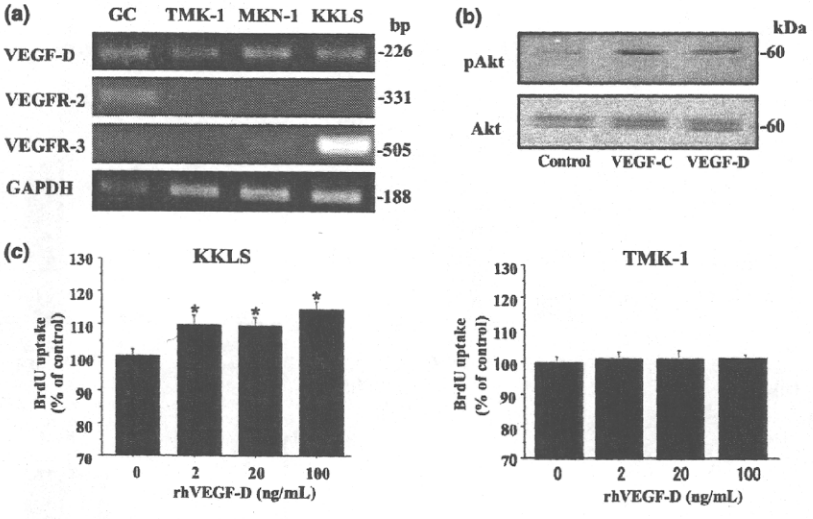

Fig. 2. Expression of VEGF-D, VEGFR-2, and VEGFR-3 in gastric carcinoma cell lines and effect of VEGF-D on KKLS cells. (a) VEGF-D, VEGFR-2, and VEGFR-3 expression by gastric carcinoma cell lines was examined by RT-PCR. Gastric cancer tissue (GC) was used for control. (b) Western blot for phosphorylation of Akt. Treatment with VEGF-C or VEGF-D induced Ser473 phosphorylation of Akt in KKLS cells. (c) KKLS and TMK-1 cells were incubated with rhVEGF-D (2, 20, or 100 ng/mL) for 24 h, and cell proliferation was measured with a cell proliferation ELISA system. *$P < 0.05$; bars, SE.

KKLS cells to grow *in vitro* was evaluated. Transfection with VEGF-D increased *in vitro* cell growth of KKLS cells (Fig. 4c). To examine the effect of VEGF-D overexpression in an animal model, we transplanted KKLS/VEGF-D and KKLS/mock cells into the gastric wall of nude mice. The mice were killed after 4 weeks, and tumors derived from KKLS/VEGF-D cells were significantly larger than KKLS/mock tumors (Fig. 4d). VEGF-D secreted by the tumor did not promote lymphatic metastasis.

Immunohistochemistry for Ki-67, CD31, and Lyve1 and *in situ* detection of apoptotic cells in KKLS cells growing in the gastric wall of nude mice. We evaluated MVD, LVD, and the Ki-67 labeling index based on immunodetection of CD31, Lyve1, and Ki-67. Indeed, statistically significant increases in MVD (Fig. 5a) and the Ki-67 labeling index (Fig. 5b) were noted in KKLS/VEGF-D tumors in comparison to those in KKLS/mock tumors. The number of lymphatic vessels was not increased in response to VEGF-D transfection (data not shown); however, the luminal area of lymphatic vessels was significantly enlarged (Fig. 5c). The apoptotic index was also evaluated. A significant decrease in the apoptotic index was noted in KKLS/VEGF-D tumors in comparison to that in KKLS/mock tumors (Fig. 5d).

Discussion

VEGF-C and VEGF-D are specific ligands for VEGFR-3 and VEGFR-2.[27,28] They have been shown to stimulate lymphangiogenesis and angiogenesis both *in vitro* and *in vivo*.[10–23] It has been reported that VEGF-D induced lymphangiogenesis in a mouse tumor model.[10,29] The expression of VEGF-D has

doi: 10.1111/j.1349-7006.2010.01649.x

Table 2. cDNA microarray analysis of KKLS cells treated with VEGF-D

Gene function	Gene symbol	Gene name	Fold change*
Cell cycle regulator	CCND1	Cyclin D1	3
	CDK4	Cyclin-dependent kinase 4	2.8
Apoptosis	BCL2	B-cell CLL/lymphoma 2	6.3
	DAPK2	Death-associated protein kinase 1	5.9
	NDUFA13	Cell death-regulatory protein GRIM19	2.8
Angiogenesis	THBS1	Thrombospondin 1	7.3
	ANG	Angiogenin, ribonuclease, RNase A family, 5	4.2
Cell adhesion	CDH1	Cadherin 1, type 1, E-cadherin (epithelial)	5.1
	ITGA7	Integrin, alpha 7	3.8
	CTNNA2	Catenin (cadherin-associated protein), alpha 2	3.6
	VIM	Vimentin	3.3
Motility, invasion	PLG	Plasminogen	10.8
	PLAUR	Plasminogen activator, urokinase receptor	4
	AMFR	Autocrine motility factor receptor	2.9

*Fold change = the degree of upregulation in comparison to expression in control (untreated) cells.

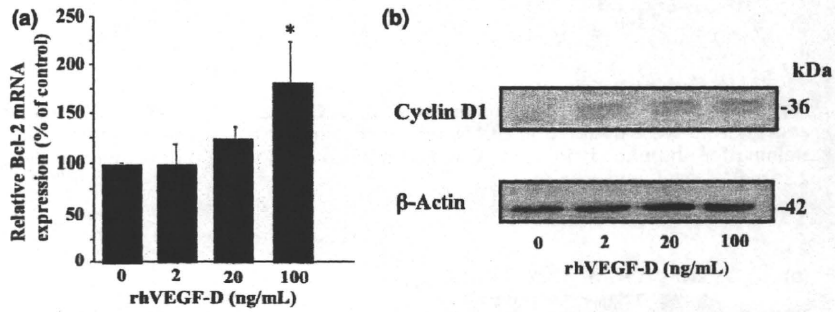

Fig. 3. KKLS cells were treated with rhVEGF-D (2, 20, or 100 ng/mL) for 8 h. Expression of (a) Bcl-2 and (b) cyclin D1 was examined by real-time PCR and western blot analysis, respectively. PCR were carried out in triplicate. Data for real-time PCR were normalized to those of β-actin. $*P < 0.05$; bars, SE.

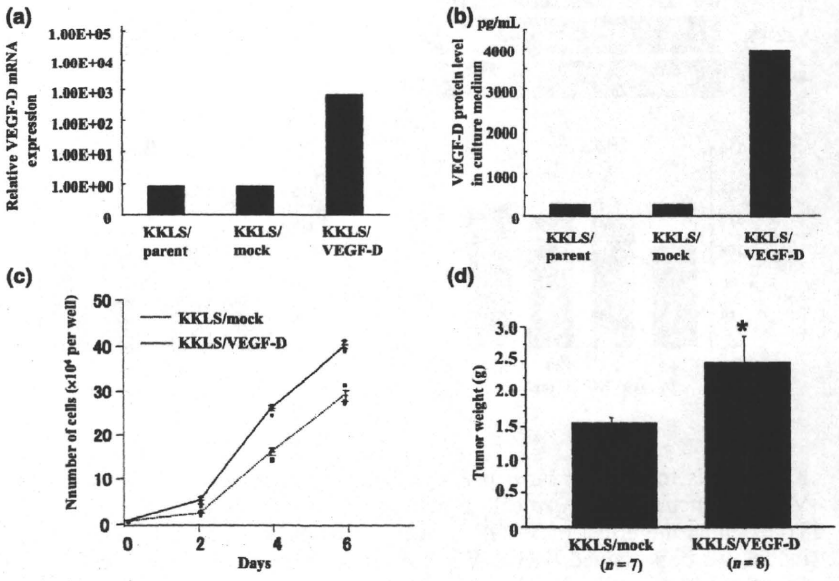

Fig. 4. Establishment of clonal cell line overexpressing VEGF-D, and *in vitro* and *in vivo* growth of VEGF-D-transfected cells. (a) Expression of VEGF-D mRNA was examined by real-time PCR. (b) VEGF-D protein level in culture medium was examined by ELISA. (c) *In vitro* cell growth of VEGF-D-transfected KKLS cells. Cells (1×10^4) were seeded in a six-well plate and cultured in RPMI-1640 containing 0.5% FBS. The number of cells was determined in triplicate cultures. (d) Orthotopic (gastric mucosa) xenograft model. Tumor weight at 4 weeks after transplantation of the VEGF-D-overexpressing clone (KKLS/VEGF-D) and corresponding vector control (KKLS/control). $*P < 0.05$; bars, SE.

been correlated with tumor lymphangiogenesis and lymph node metastasis in many human carcinomas, including breast,[14] lung,[19] gastric,[18] and colorectal cancers.[13] We previously examined expression of VEGF-C and VEGF-D by immunohistochemistry in 140 archival surgical specimens of submucosally invasive gastric carcinoma. VEGF-C immunoreactivity was associated with histologic type, lymphatic invasion, lymph node metastasis, and MVD. There was no association between VEGF-D immunoreactivity and clinicopathologic features. These results suggest that VEGF-C is the dominant regulator of lymphangiogenesis in early stage human gastric carcinoma.[22]

VEGFR-3 has also been detected in several types of malignant cells,[30,31] although it is mainly expressed by lymphatic endothelial cells. In various types of cancer cells, autocrine VEGF-A/VEGFR-2 loops on tumor cells regulate their growth and survival.[32–34] We and others have reported the existence of autocrine stimulation of tumor growth via the VEGF-C/VEG-

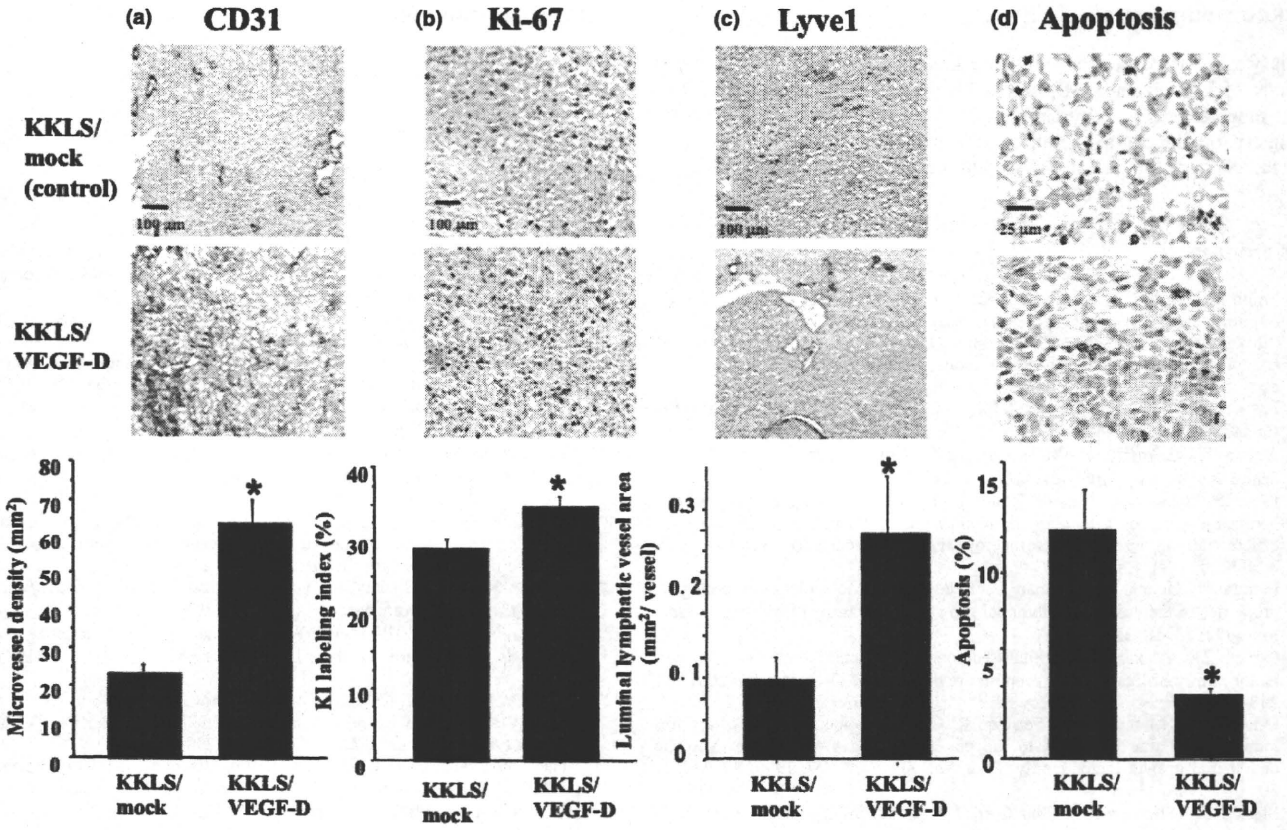

Fig. 5. Immunohistochemistry for (a) CD31, (b) Ki-67, and (c) Lyve1, and (d) *in situ* detection of apoptotic cells in KKLS cells growing in the gastric wall of nude mice. Lower panels, quantification of CD31-positive vessels, Ki-67-positive cells, Lyve1-positive vessels, and apoptotic cells. Scale bars: (a,c) 200 μm. *$P < 0.05$; bars, SE.

FR-3 axis in lung,[30] breast,[31] and gastric cancers.[24] In the present study, we examined the expression of VEGF-D and VEGFR-3 in human gastric carcinomas and the role of the VEGF-D/VEGFR-3 axis in tumor cells. In 10 of 29 (34%) gastric carcinoma specimens, tumor cells expressed both VEGF-D and VEGFR-3. Treatment of KKLS cells (VEGFR-3-expressing cell line) with recombinant VEGF-D induced tyrosine phosphorylation of VEGFR-3 and Akt, indicating that VEGFR-3 on tumor cells is functional. Microarray analysis showed up-regulation of cyclin D1 (cell cycle regulator) and Bcl-2 (anti-apoptotic protein) by treatment with VEGF-D. We reported previously that treatment with VEGF-C induced phosphorylation of VEGFR-3 and Akt and increased expression of cyclin D1, PlGF, autocrine motility factor (AMF), and AMF receptor by KKLS cells.[24] Makinen *et al.*[35] showed that VEGFR-3 signaling induces protein kinase C (PKC)-dependent p42/p44 MAPK activation and wortmannin-sensitive phosphorylation of Akt. These findings suggest that VEGF-C and VEGF-D are associated with cell proliferation and survival via these signaling cascades in tumor cells.

To stimulate VEGF-D/VEGFR-3 signaling in an autocrine manner, VEGF-D expression vector was transfected into KKLS cells (KKLS/VEGF-D cells), and these cells were then transplanted into the gastric wall of nude mice. It has been reported that binding of VEGF-D to VEGFR-3 on the lymphatic endothelial cells resulted in dilatation of existing lymphatic vessels as well as in vegetation of new vessels.[36] In the present study, the luminal area of lymphatic vessels was increased in KKLS/VEGF-D tumors in comparison to that in control (KKLS/mock) tumors, indicating that the KKLS/VEGF-D cells produce functional VEGF-D protein. However, VEGF-D secreted by the tumor did not promote lymphatic metastasis. In contrast, Stacker *et al.*[10] reported that expression of VEGF-D in tumor cells led to spread of the tumor to lymph nodes. These discrepancies may be due to differences in cell lines and experimental animal models. Lymphatic metastasis is the consequence of a complex metastatic process, which includes lymphangiogenesis,[37,38] dissemination, transport, settlement, and growth in the lymphatic system. These involve not only VEGF-D but many other growth factors such as VEGF-C, angiopoietins, fibroblast growth factor, and platelet-derived growth factor.[39]

In vitro treatment with VEGF-D increased expression of cyclin D1 and stimulated proliferation of KKLS cells. The Ki-67 labeling index and tumor weight increased in orthotopic KKLS/VEGF-D tumors in comparison to those in orthotopic KKLS/mock tumors. These increases were associated with increased MVD, indicating that VEGF-D transfection into KKLS cells stimulates angiogenesis. In addition, we found that *in vitro* treatment with VEGF-D increased expression of Bcl-2, a key regulator of apoptotic inhibition. The number of apoptosis cells was lower in KKLS/VEGF-D tumors than in KKLS/mock tumors. Consistent with our results, Akahane *et al.*[40] reported that overexpression of VEGF-D in breast cancer cell lines resulted in up-regulation of the *Bcl-2* gene.

In conclusion, human gastric carcinoma cells express VEGF-D as well as VEGFR-3. VEGF-D may be involved in the progression of human gastric carcinoma not only by stimulating angiogenesis and lymphangiogenesis via a paracrine mechanism, but also by regulating cell proliferation and apoptosis via an autocrine mechanism. Further studies are needed to identify precise signaling mechanisms responsible for the autocrine role of VEGF-D.

doi: 10.1111/j.1349-7006.2010.01649.x

Acknowledgments

This work was carried out with the kind cooperation of the Analysis Center of Life Science, Hiroshima University (Hiroshima, Japan) and was supported, in part, by Grants-in-Aid for Cancer Research from the Ministry of Education, Culture, Science, Sports and Technology of Japan, and from the Ministry of Health, Labor and Welfare of Japan.

Disclosure Statement

The authors have no conflict of interest.

References

1 Smith MG, Hold GL, Tahara E, El-Omar EM. Cellular and molecular aspects of gastric cancer. *World J Gastroenterol* 2006; **12**: 2979–90.
2 Stacker SA, Achen MG, Jussila L, Baldwin ME, Alitalo K. Lymphangiogenesis and cancer metastasis. *Nat Rev Cancer* 2002; **2**: 573–83.
3 Ferrara N. VEGF and the quest for tumour angiogenesis factors. *Nat Rev Cancer* 2002; **2**: 795–803.
4 Alitalo K, Carmeliet P. Molecular mechanisms of lymphangiogenesis in health and disease. *Cancer Cell* 2002; **1**: 219–27.
5 Berse B, Brown LF, Van de Water L, Dvorak HF, Senger DR. Vascular permeability factor (vascular endothelial growth factor) gene is expressed differentially in normal tissues, macrophages, and tumors. *Mol Biol Cell* 1992; **3**: 211–20.
6 Ferrara N, Houck K, Jakeman L, Leung DW. Molecular and biological properties of the vascular endothelial growth factor family of proteins. *Endocr Rev* 1992; **13**: 18–32.
7 Otrock ZK, Makarem JA, Shamseddine AI. Vascular endothelial growth factor family of ligands and receptors: review. *Blood Cells Mol Dis* 2007; **38**: 258–68.
8 Orlandini M, Marconcini L, Ferruzzi R, Oliviero S. Identification of a c-fos-induced gene that is related to the platelet-derived growth factor/vascular endothelial growth factor family. *Proc Natl Acad Sci USA* 1996; **93**: 11675–80.
9 Stacker SA, Stenvers K, Caesar C *et al.* Biosynthesis of vascular endothelial growth factor-D involves proteolytic processing which generates non-covalent homodimers. *J Biol Chem* 1996; **274**: 32127–36.
10 Stacker SA, Caesar C, Baldwin ME *et al.* VEGF-D promotes the metastatic spread of tumor cells via the lymphatics. *Nat Med* 2001; **7**: 186–91.
11 Thelen A, Scholz A, Benckert C *et al.* VEGF-D promotes tumor growth and lymphatic spread in a mouse model of hepatocellular carcinoma. *Int J Cancer* 2008; **122**: 2471–81.
12 Von Marschall Z, Scholz A, Stacker SA *et al.* Vascular endothelial growth factor-D induces lymphangiogenesis and lymphatic metastasis in models of ductal pancreatic cancer. *Int J Oncol* 2005; **27**: 669–79.
13 White JD, Hewett PW, Kosuge D *et al.* Vascular endothelial growth factor-D expression is an independent prognostic marker for survival in colorectal carcinoma. *Cancer Res* 2002; **62**: 1669–75.
14 Nakamura Y, Yasuoka H, Tsujimoto M *et al.* Prognostic significance of vascular endothelial growth factor D in breast carcinoma with long-term follow-up. *Clin Cancer Res* 2003; **9**: 716–21.
15 Kurahara H, Takao S, Maemura K, Shinchi H, Natsugoe S, Aikou T. Impact of vascular endothelial growth factor-C and -D expression in human pancreatic cancer: its relationship to lymph node metastasis. *Clin Cancer Res* 2004; **10**: 8413–20.
16 Yokoyama Y, Charnock-Jones DS, Licence D *et al.* Vascular endothelial growth factor-D is an independent prognostic factor in epithelial ovarian carcinoma. *Br J Cancer* 2003; **88**: 237–44.
17 Yokoyama Y, Charnock-Jones DS, Licence D *et al.* Expression of vascular endothelial growth factor (VEGF)-D and its receptor, VEGF receptor 3, as a prognostic factor in endometrial carcinoma. *Clin Cancer Res* 2003; **9**: 1361–9.
18 Jüttner S, Wissmann C, Jöns T *et al.* Vascular endothelial growth factor-D and its receptor VEGFR-3: two novel independent prognostic markers in gastric adenocarcinoma. *J Clin Oncol* 2006; **24**: 228–40.
19 Niki T, Iba S, Tokunou M, Yamada T, Matsuno Y, Hirohashi S. Expression of vascular endothelial growth factors A, B, C, and D and their relationships to lymph node status in lung adenocarcinoma. *Clin Cancer Res* 2000; **6**: 2431–9.
20 O-charoenrat P, Rhys-Evans P, Eccles SA. Expression of vascular endothelial growth factor family members in head and neck squamous cell carcinoma correlates with lymph node metastasis. *Cancer* 2001; **92**: 556–68.
21 George ML, Tutton MG, Janssen F *et al.* VEGF-A, VEGF-C, and VEGF-D in colorectal cancer progression. *Neoplasia* 2001; **3**: 420–7.
22 Onogawa S, Kitadai Y, Tanaka S, Kuwai T, Kimura S, Chayama K. Expression of VEGF-C and VEGF-D at the invasive edge correlates with lymph node metastasis and prognosis of patients with colorectal carcinoma. *Cancer Sci* 2004; **95**: 32–9.
23 Kitadai Y, Kodama M, Cho S *et al.* Quantitative analysis of lymphangiogenic markers for predicting metastasis of human gastric carcinoma to lymph nodes. *Int J Cancer* 2005; **115**: 388–92.
24 Kodama M, Kitadai Y, Tanaka M *et al.* Vascular endothelial growth factor C stimulates progression of human gastric cancer via both autocrine and paracrine mechanism. *Clin Cancer Res* 2008; **14**: 7205–14.
25 Japanese Research Society for Gastric Cancer. *Japanese Classification of Gastric Carcinoma*. Kanehara & Co., Tokyo, 1999.
26 Weidner N, Semple JP, Welch WR, Folkman J. Tumor angiogenesis and metastasis: correlation in invasive breast carcinoma. *N Engl J Med* 1991; **324**: 1–8.
27 Joukov V, Pajusola K, Kaipainen A *et al.* A novel vascular endothelial growth factor, VEGF-C, is a ligand for the Flt4 (VEGFR-3) and KDR (VEGFR-2) receptor tyrosine kinases. *EMBO J* 1996; **15**: 290–8.
28 Achen MG, Jeltsch M, Kukk E *et al.* Vascular endothelial growth factor D (VEGF-D) is a ligand for the tyrosine kinases VEGF receptor 2 (Flk1) and VEGF receptor 3 (Flt4). *Proc Natl Acad Sci USA* 1998; **95**: 548–53.
29 Kopfstein L, Veikkola T, Djonov VG *et al.* Distinct roles of vascular endothelial growth factor-D in lymphangiogenesis and metastasis. *Am J Pathol* 2007; **170**: 1348–61.
30 Tanno S, Ohsaki Y, Nakanishi K, Toyoshima E, Kikuchi K. Human small cell lung cancer cells express functional VEGF receptors, VEGFR-2 and VEGFR-3. *Lung Cancer* 2004; **46**: 11–19.
31 Timoshenko AV, Rastogi S, Lala PK. Migration-promoting role of VEGF-C and VEGF-C binding receptors in human breast cancer cells. *Br J Cancer* 2007; **97**: 1090–8.
32 Von Marschall Z, Cramer T, Höcker M *et al.* De novo expression of vascular endothelial growth factor in human pancreatic cancer: evidence for an autocrine mitogenic loop. *Gastroenterology* 2000; **119**: 1358–72.
33 Bachelder RE, Wendt MA, Mercurio AM. Vascular endothelial growth factor promotes breast carcinoma invasion in an autocrine manner by regulating the chemokine receptor CXCR4. *Cancer Res* 2002; **62**: 7203–6.
34 Jackson MW, Roberts JS, Heckford SE *et al.* A potential autocrine role for vascular endothelial growth factor in prostate cancer. *Cancer Res* 2002; **62**: 854–9.
35 Mäkinen T, Veikkola T, Mustjoki S *et al.* Isolated lymphatic endothelial cells transduce growth, survival and migratory signals via the VEGF-C/D receptor VEGFR-3. *EMBO J* 2002; **20**: 4762–73.
36 Veikkola T, Jussila L, Makinen T *et al.* Signalling via vascular endothelial growth factor receptor-3 is sufficient for lymphangiogenesis in transgenic mice. *EMBO J* 2001; **20**: 1223–31.
37 Achen MG, McColl BK, Stacker SA. Focus on lymphangiogenesis in tumor metastasis. *Cancer Cell* 2005; **7**: 121–7.
38 Karpanen T, Alitalo K. Lymphatic vessels as targets of tumor therapy? *J Exp Med* 2001; **194**: F37–42.
39 Folkman J. Looking for a good endothelial address. *Cancer Cell* 2002; **1**: 113–15.
40 Akahane M, Akahane T, Matheny SL, Shah A, Okajima E, Thorgeirsson UP. Vascular endothelial growth factor-D is a survival factor for human breast carcinoma cells. *Int J Cancer* 2006; **118**: 841–9.

Expression of platelet-derived growth factor (PDGF)-B and PDGF-receptor β is associated with lymphatic metastasis in human gastric carcinoma

Michiyo Kodama,[1] Yasuhiko Kitadai,[1,4] Tomonori Sumida,[1] Mayu Ohnishi,[1] Eiji Ohara,[1] Miwako Tanaka,[1] Kei Shinagawa,[1] Shinji Tanaka,[2] Wataru Yasui[3] and Kazuaki Chayama[1]

[1]Department of Medicine and Molecular Science, Hiroshima University Graduate School of Biomedical Sciences, Hiroshima; [2]Department of Endoscopy, Hiroshima University Hospital, Hiroshima; [3]Department of Pathology, Hiroshima University Graduate School of Biomedical Sciences, Hiroshima, Japan

(Received March 15, 2010/Revised May 25, 2010/Accepted May 28, 2010/Accepted manuscript online June 7, 2010/Article first published online July 7, 2010)

Recent study of murine fibrosarcoma has revealed that platelet-derived growth factor (PDGF) plays a direct role in promoting lymphangiogenesis and metastatic spread to lymph nodes. Thus, we investigated the relation between PDGF and PDGF receptor (PDGF-R) expression and lymphatic metastasis in human gastric carcinoma. We examined PDGF-B and PDGF-Rβ expression in four human gastric carcinoma cell lines (TMK-1, MKN-1, MKN-45, and KKLS) and in 38 surgical specimens of gastric carcinoma. PDGF-B and PDGF-Rβ expression was examined by immunofluorescence in surgical specimens and in human gastric carcinoma cells (TMK-1) implanted orthotopically in nude mice. Groups of mice (n = 10, each) received saline (control) or PDGF-R tyrosine kinase inhibitor imatinib. PDGF-B and PDGF-Rβ mRNA expression was significantly higher in patients with lymph node metastasis than in those without and was also significantly higher in diffuse-type carcinoma than in intestinal-type carcinoma. In surgical specimens, tumor cells expressed PDGF-B, but PDGF-Rβ was expressed predominantly by stromal cells. Under culture conditions, expression of PDGF-B mRNA was found in all of the gastric cell lines, albeit at different levels. In orthotopic TMK-1 tumors, cancer cells expressed PDGF-B but not PDGF-Rβ. PDGF-Rβ was expressed by stromal cells, including lymphatic endothelial cells. Four weeks of treatment with imatinib significantly decreased the area of lymphatic vessels. Our data indicate that secretion of PDGF-B by gastric carcinoma cells and expression of PDGF-Rβ by tumor-associated stromal cells are associated with lymphatic metastasis. Blockade of PDGF-R signaling pathways may inhibit lymph node metastasis of gastric carcinoma. (*Cancer Sci* 2010; 101: 1984–1989)

Gastric cancer is one of the most frequent malignancies in the world. The major cause of mortality is metastasis, which relies on *de novo* formation of blood and lymphatic vessels.[1] Although induction of tumor angiogenesis is known to be a complex process that involves the interplay of a dozen or more tumor-derived growth factors,[2] how tumors induce lymphangiogenesis is poorly understood.

Among known lymphangiogenic factors, the best-characterized growth factors are vascular endothelial growth factor C (VEGF-C) and VEGF-D.[3–8] Fibroblast growth factor-2 promotes lymphatic vessel growth in the mouse cornea, but this effect is believed to occur indirectly, via induction of VEGF-C expression and activation of VEGF receptor 3 (VEGFR-3) signaling.[9] It is unlikely that VEGF-C and -D and VEGFR-3 are the sole factors regulating such processes. A range of lymphangiogenic factors produced by tumor cells, endothelial cells, and stromal cells has recently been identified. These include VEGF-A, and members of the hepatocyte growth factor (HGF) and angiopoietin (Ang) families.[10–12] Additionally, interesting preclinical studies have indicated that platelet-derived growth factors (PDGFs) and PDGF receptors (PDGF-Rs) not only promote hemangiogenesis and direct tumor cell growth but are important players in lymphangiogenesis.[13]

Members of the PDGF family are often expressed at high levels in many malignant tissues.[14] The PDGF family consists of five isoforms, -AA, -AB, -BB, -CC, and -DD, usually referred to as PDGF-A (AA), PDGF-B (AB and BB), PDGF-C (CC), and PDGF-D (DD).[15] Their biological activities are mediated by three forms of the tyrosine kinase receptor encoded by two gene products, PDGF-Rα and -Rβ. PDGF-Rα binds all possible forms of PDGF except PDGF-DD, whereas PDGF-Rβ preferentially binds PDGF-BB.[16] PDGFs have been found to induce tumor growth by directly stimulating growth of certain types of tumor cells,[17] to stimulate angiogenesis,[18] to recruit pericytes[19] and to control the interstitial fluid pressure in stroma, influencing transvascular transport of chemotherapeutic agents in a paracrine manner.[20] Recently, Cao *et al.*[13] showed that expression of PDGF-B in murine fibrosarcoma cells induced tumor lymphangiogenesis, leading to enhanced lymph node metastasis. However, there is no report concerning the relation between PDGF-B and PDGF-Rβ expression and lymphatic metastasis in human gastric carcinoma. Thus, we examined the expression profile of PDGF-B and PDGF-Rβ in human gastric carcinoma, and we examined whether blocking PDGF-R can inhibit lymphangiogenesis of gastric cancer *in vivo*.

Materials and Methods

Patients and tumor specimens. Endoscopic biopsy specimens (tumor and corresponding normal mucosa) of gastric tissue from 38 patients with gastric carcinoma who later underwent surgical resection at Hiroshima University Hospital were snap-frozen in liquid nitrogen and stored at −80°C until RNA extraction for quantitative RT-PCR. Informed consent was obtained from all patients for participation in the study according to the Declaration of Helsinki. Pathology reports and clinical histories were reviewed for accurate staging at the time of surgery. Criteria for staging and histologic classification were those proposed by the Japanese Research Society for Gastric Cancer.[21] Lymph node status was determined by routine pathological examination with the surgical specimens. Two groups of patients, those with lymph node metastasis (node-positive group, n = 21) and those without (node-negative group, n = 17), were closely matched for histologic type and depth of invasion. The patient group comprised 34 men and four women with a median age of

[4]To whom correspondence should be addressed.
E-mail: kitadai@hiroshima-u.ac.jp

doi: 10.1111/j.1349-7006.2010.01639.x

66.5 years. All patients had invasive gastric carcinoma in which the tumor invasion was beyond the submucosa.

Cell cultures. Four cell lines established from human gastric carcinomas and human osteosarcoma cell line MG63 were maintained in RPMI-1640 (Nissui, Tokyo, Japan) with 10% fetal bovine serum (FBS; MA BioProducts, Baltimore, MD, USA). TMK-1 cell line (a poorly differentiated adenocarcinoma) was provided by Dr E. Tahara of Hiroshima University. KKLS cell line (an undifferentiated carcinoma) was provided by Dr Y. Takahashi of Chiba University, Chiba, Japan. Two other cell lines (MKN-1, from an adenosquamous carcinoma, and MKN-45, from a poorly differentiated adenocarcinoma) as well as MG63 were obtained from the Health Science Research Resources Bank, Osaka, Japan.

Quantitative real-time RT-PCR analysis. Total RNA was extracted from gastric carcinoma cell lines and biopsy specimens with an RNeasy Kit (Qiagen, Valencia, CA, USA) according to the manufacturer's instructions. cDNA was synthesized from 1 μg total RNA with a first-strand cDNA synthesis kit (Amersham Biosciences, Piscataway, NJ, USA). After reverse transcription of RNA into cDNA, quantitative RT-PCR was performed with a LightCycler-FastStart DNA Master SYBR-Green I Kit (Roche Diagnostics, Basel, Switzerland) according to the manufacturer's recommended protocol. Polymerase chain reaction (PCR) reactions were carried out in triplicate. To correct for differences in both RNA quality and quantity between samples, values were normalized to those of β-actin. The mRNA ratio between gastric carcinoma tissues (T) and corresponding normal mucosa (N) was calculated and expressed as the T/N ratio. Primers for PCR were designed with specific primer analysis software (Primer Designer; Scientific and Educational Software, Durham, NC, USA), and specificity of the sequences was confirmed by FASTA (EMBL Database). Respective primer sequences, annealing temperatures, and PCR cycles were as follows: PDGF-B forward, CGAGTTGGACCTGAACATGA and PDGF-B reverse, GTCACCGTGGCCTTCTTAAA (PDGF-B PCR product, 339 bp; 58°C; 35 cycles); PDGF-Rβ forward, AGCTACCCCTCAAGGAATCATAG and PDGF-Rβ reverse, CTCTGGTGGATGGATTAAGACTG (PDGF-Rβ PCR product, 376 bp; 58°C; 35 cycles); and GAPDH forward, ATCATCCCTGCCTCTACTGG and GAPDH reverse, CCCTCCGACGCCTGCTTCAC (GAPDH PCR product, 188 bp; 55°C; 28 cycles).

Reagents. Imatinib (imatinib mesylate or Gleevec; Novartis Pharma, Basel, Switzerland) is a 2-phenylaminopyrimidine class protein-tyrosine kinase inhibitor of PDGF-R, BCR–ABL, and c-Kit.[22,23] Imatinib was diluted in sterile water for oral administration. Primary antibodies were purchased from as follows: polyclonal rabbit anti-PDGF-Rβ and polyclonal rabbit anti-PDGF-B subunit from Santa Cruz Biotechnology (Santa Cruz, CA, USA); and rat antimouse Lyve-1 from R&D Systems (Minneapolis, MN, USA).

Western blot analysis. After three washes with cold phosphate-buffered saline (PBS) containing 1 mmol/L sodium orthovanadate, cells were lysed. Proteins (total protein 20 μg) were separated by SDS-PAGE and transferred to nitrocellulose transfer membranes (Whatman, Dassel, Germany). The immune complexes were visualized by enhanced chemiluminescence with an ECL Plus Kit (GE Healthcare, Buckinghamshire, UK).

Animals and orthotopic implantation of tumor cells. Male athymic BALB/c nude mice were obtained from Charles River Japan (Tokyo, Japan). The mice were maintained under specific pathogen-free conditions and used at 5 weeks of age. This study was carried out after permission was granted by the Committee on Animal Experimentation of Hiroshima University.

Subconfluent gastric cancer cells (TMK-1 or KKLS cells) to be used for implantation were harvested by brief treatment with 0.25% trypsin and 0.02% ethylenediamine tetraacetic acid, and then resuspended to a final concentration of 2.0×10^7 cells/mL Hanks' solution. With the use of a 30-gauge needle attached to a 1-mL syringe, cells (1×10^6 cells in 50 μL) were implanted into the gastric walls in the nude mice under observation with a zoom stereomicroscope. After 4 weeks, the mice were killed, and the tumors were resected for study. The tumors were embedded in OCT compound (Miles, Elkhart, IN, USA), rapidly frozen in liquid nitrogen, and stored at −80°C.

Immunofluorescence staining for PDGF-B and PDGF-Rβ, and double staining for PDGF-Rβ and Lyve-1. Fresh frozen specimens of human gastric carcinomas as well as human gastric carcinomas growing in nude mice were cut into 8-μm sections, mounted on positively charged slides, and stored at −80°C. Tissue sections were fixed in cold acetone for 10 min and then washed three times with PBS for 3 min each. Slides were placed in a humidified chamber and incubated with protein blocking solution (5% normal horse serum and 1% normal goat serum in PBS) for 20 min at room temperature. The slides were incubated overnight at 4°C with primary antibody against PDGF-B or PDGF-Rβ, then rinsed three times with PBS, incubated for 10 min in protein blocking solution, and incubated for 1 h at room temperature with Cy3-conjugated goat antirabbit secondary antibody. From this point onwards, the slides were protected from light. The samples were then rinsed three times in PBS. To identify lymph endothelial cells, slides were incubated overnight at 4°C with antibody against Lyve-1. The sections were rinsed three times with PBS and incubated for 10 min in protein blocking solution. Slides were then incubated for 1 h at room temperature with corresponding Cy5-conjugated secondary antibody, and the samples were rinsed three times in PBS. 4′,6-diamidino-2-phenylindole (DAPI) nuclear counterstain was applied for 10 min. Samples were then rinsed three times with PBS, and mounting medium was placed on each sample, which was then covered with a glass coverslip. We used Fluoromount/Plus (Diagnostic Bio Systems, Pleasanton, CA, USA) as the mounting medium.

Confocal microscopy. Confocal fluorescence images were obtained at ×203 or ×403 magnification on a Zeiss LSM 510 laser scanning microscopy system (Carl Zeiss, Thornwood, NY, USA) equipped with a motorized Axioplan microscope, argon laser (458/477/488/514 nm, 30 mW), HeNe lasers (543 nm, 1 mW; 633 nm, 5 mW), LSM 510 control and image acquisition software, and appropriate filters (Chroma Technology, Brattleboro, VT, USA). Confocal images were exported to Adobe Photoshop (Adobe Systems, San Jose, CA, USA), and photo montages were prepared for publication. Lymphatic endothelial cells were identified by green fluorescence, whereas PDGF and PDGF-R were identified by red fluorescence.

Treatment of established human gastric cancer tumors growing in murine gastric walls. Fourteen days after orthotopic

Table 1. Results of quantitative real-time PCR for mRNA expression of PDGF-B and PDGF-Rβ of human gastric carcinoma specimens

	PDGF-Rβ		PDGF-B	
Lymph node status				
Node-positive (n = 21)	6.46 ± 1.45	P = 0.0001	5.06 ± 1.88	P = 0.027
Node-negative (n = 17)	0.97 ± 0.29		0.95 ± 0.18	
Histologic type				
Intestinal (n = 22)	1.32 ± 0.42	P = 0.0041	1.54 ± 0.71	P = 0.028
Diffuse (n = 16)	5.45 ± 1.33		5.02 ± 2.16	

PDGF-B, platelet-derived growth factor B; PDGF-Rβ, PDGF receptor β.

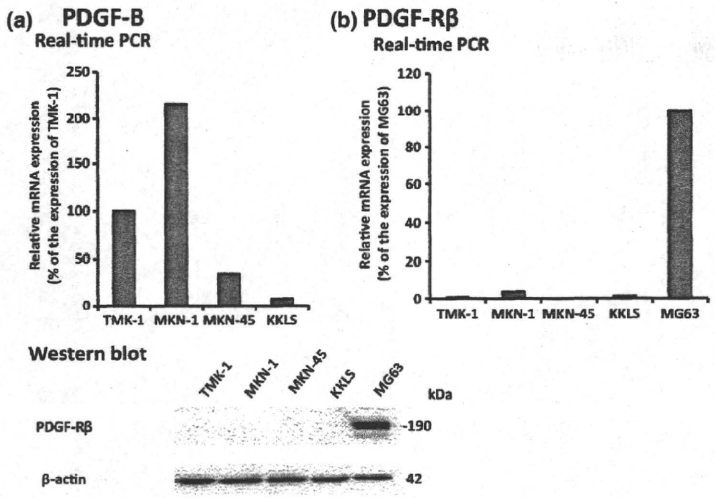

Fig. 1. Expression of platelet-derived growth factor B (PDGF-B) and PDGF receptor β (PDGF-Rβ) in gastric carcinoma cell lines. (a) Gastric cancer cell lines constitutively expressed mRNA for PDGF-B subunit at various levels. (b) PDGF-Rβ was not expressed by the cultured gastric carcinoma cell lines.

implantation of TMK-1 cells, mice (n = 10 each group) were randomly assigned to receive one of the following two treatments: daily oral gavage of water (control group) or daily oral gavage of imatinib (50 mg/kg, optimal biological dose as determined previously[17,24]). The treatments continued for 28 days. All therapy experiments were performed twice. The mice bearing orthotopic tumors were euthanized by methophane on day 29. For immunohistochemistry, the tumor tissues were fixed in formalin and embedded in paraffin.

Immunohistochemical determination of the area of lymphatic vessels. Paraffin-embedded tissues were used for immunohistochemical identification of Lyve-1. Sections were deparaffinized and rehydrated in PBS, microwaved in water for 5 min for antigen retrieval, incubated overnight at 4°C with mouse anti-Lyve-1 antibody, and incubated for 1 h at room temperature with a peroxidase-conjugated rat antimouse antibody. A positive reaction was detected by exposure to stable 3,3′-diaminobenzidine for 5–10 min. Slides were counterstained with Gill's hematoxylin. On slides immunolabeled for Lyve-1, only vessels with typical morphology (including a lumen) were counted as lymphatic vessels because of occasional weak antibody cross-reactivity with fibroblasts.[25] For quantification of the lymphatic vessel areas, 10 random fields at ×100 magnification were captured for each tumor, and the outline of each lymphatic vessel including a lumen was manually traced. The areas were then calculated with the use of NIH ImageJ software (http://rsbweb.nih.gov/ij/download.html).

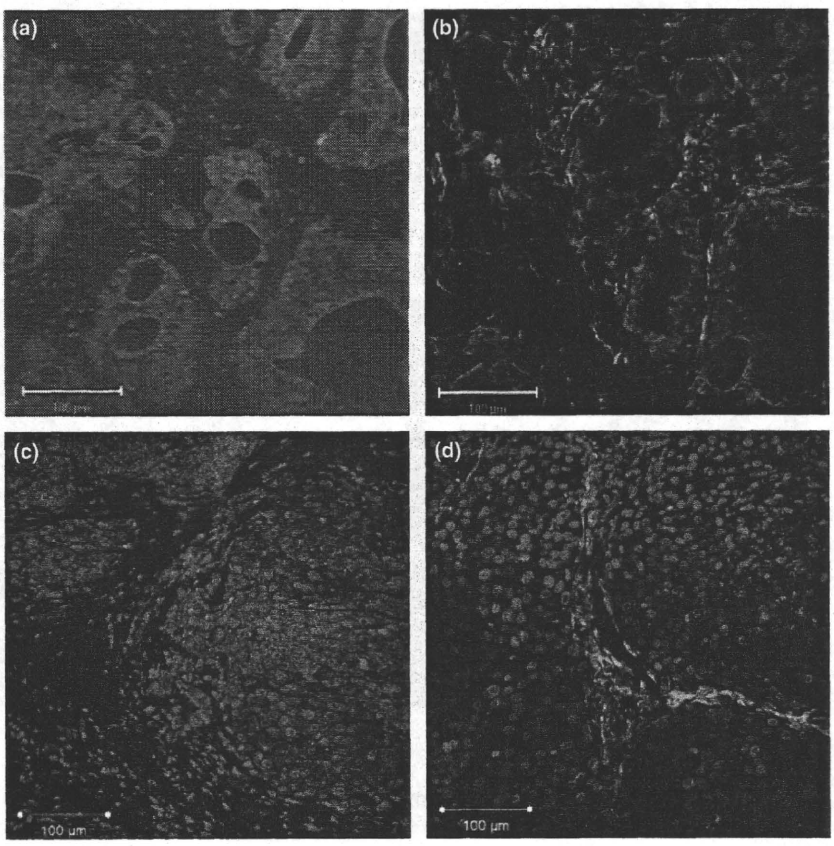

Fig. 2. Immunohistochemical detection of platelet-derived growth factor B (PDGF-B) and PDGF receptor β (PDGF-Rβ) in gastric carcinoma. (a,b) Immunolocalization of PDGF-B and PDGF-Rβ in human gastric carcinoma tissues. (c,d) Immunolocalization of PDGF-B and PDGF-Rβ in an orthotopic xenograft model (TMK-1 cell line). Expression of PDGF-B (a,c) and PDGF-Rβ (b,d) in tumor tissue appears red.

doi: 10.1111/j.1349-7006.2010.01639.x

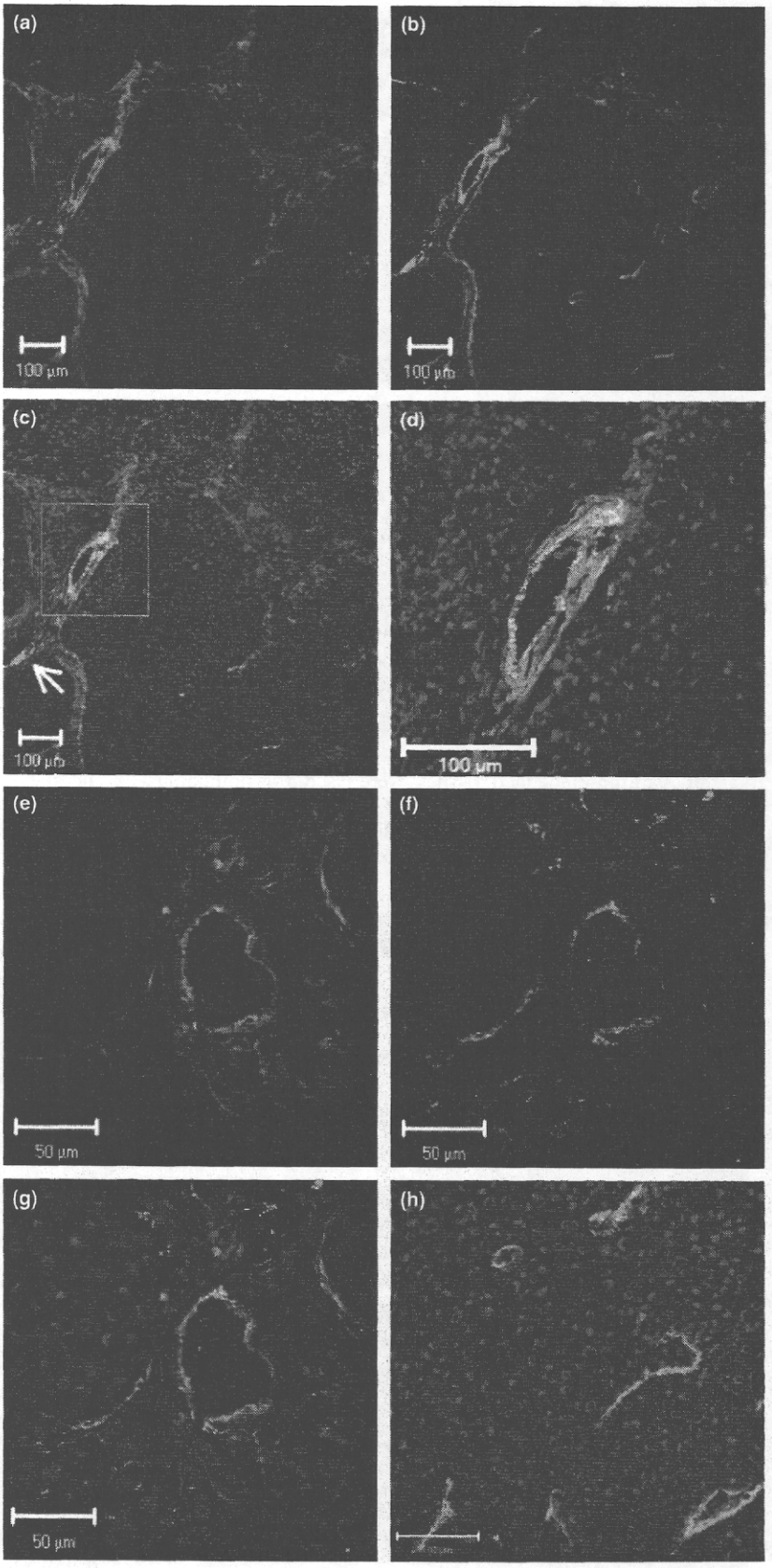

Fig. 3. Fluorescence double-labeled immunohistochemistry (IHC) of TMK-1 human gastric cancer cells growing in nude mice. Representative images show IHC for PDGF-Rβ in red and Lyve-1 (lymphatic endothelial marker) in green. (a–g) PDGF-Rβ was detected in lymphatic endothelial cells on enlarged and tortuous lymphatic vessels located immediately adjacent to tumor nests. Small lymphatic vessels (arrow) did not express PDGF-Rβ. (h) Intratumoral lymphatic vessels did not express PDGF-Rβ.

Statistical analysis. Results are expressed as mean ± SE. Wilcoxon/Kruskal–Wallis analysis was used to analyze between-group differences in continuous variables. A P-value of <0.05 was considered statistically significant.

Results

Expression levels of PDGF-B and PDGF-Rβ mRNAs in human gastric carcinoma. We initially examined mRNA expression of

PDGF-B and PDGF-Rβ by quantitative real-time PCR. The relative expression levels (T/N ratio) of PDGF-B and PDGF-Rβ are shown according to node status in Table 1. Patients with positive lymph nodes showed significantly greater expression of PDGF-B and PDGF-Rβ than node-negative patients ($P = 0.03$ and $P < 0.001$, respectively). We also examined the relation between PDGF-B and PDGF-Rβ mRNA expression and histologic type of human gastric carcinoma because diffuse-type gastric carcinoma is known to have abundant stroma and a high probability of lymph node metastasis. Expression of PDGF-B and PDGF-Rβ was significantly greater in patients with diffuse-type gastric carcinoma than in those with intestinal-type gastric carcinoma ($P = 0.03$ and $P = 0.004$, respectively) (Table 1).

Expression of PDGF-B and PDGF-Rβ in human gastric carcinoma cell lines growing in culture. We examined expression of PDGF-B and PDGF-Rβ in four human gastric carcinoma cell lines derived from different histological types. MG63 cells were used as a positive control for PDGF-R expression. The results of real-time PCR and western blot analysis are shown in Figure 1. Under culture conditions, expression of PDGF-B mRNA was found in all of the gastric cell lines, albeit at different levels. PDGF-Rβ was not expressed by the cultured gastric carcinoma cell lines.

Immunolocalization of PDGF-B and PDGF-Rβ in human gastric carcinoma tissues and in human gastric carcinoma cells growing in the mouse stomachs. We next confirmed PDGF-B and PDGF-Rβ expression *in vivo*. We used TMK-1 and KKLS cells for animal models because the other cell lines (MKN-1 and MKN-45) were difficult to grow in the mouse gastric walls. Representative photomicrographs are shown in Figure 2. Because TMK-1 tumors had more abundant stroma than KKLS tumors, it was convenient to use TMK-1 tumors to evaluate PDGF-B and PDGF-Rβ expression in stroma. In the surgical specimens and the orthotopic xenograft models, tumor cells expressed PDGF-B, but PDGF-Rβ was expressed predominantly by stromal cells (Fig. 2a–d).

Immunohistochemical analysis of PDGF-Rβ and Lyve-1 expression in TMK-1 tumors. To identify whether tumor-associated lymphatic vessels express PDGF-Rβ, we analysed co-localization of PDGF-Rβ and Lyve-1 (lymphatic endothelial cells). Co-localization of green (Lyve-1) and red (PDGF-Rβ) fluorescence appeared as yellow fluorescence, indicating that tumor-associated lymphatic vessels expressed PDGF-Rβ. PDGF-Rβ was expressed occasionally on lymphatic endothelial cells, especially on enlarged and tortuous lymphatic vessels located immediately adjacent to tumor nests (Fig. 3a–g). Lymphatic vessels in normal tissue or intratumoral lymphatic vessels did not express PDGF-Rβ (Fig. 3h).

Treatment of human gastric carcinoma growing in mouse stomachs. We determined the effects of imatinib, PDGF-Rβ thyrosine kinase inhibitor, on lymphatic vessels in tumors growing up from implantation of TMK-1 human gastric carcinoma cells into the stomachs of nude mice. The tumors treated with imatinib had reduced areas of lymphatic vessels in comparison to areas of lymphatic vessels in control tumors ($P < 0.05$) (Fig. 4).

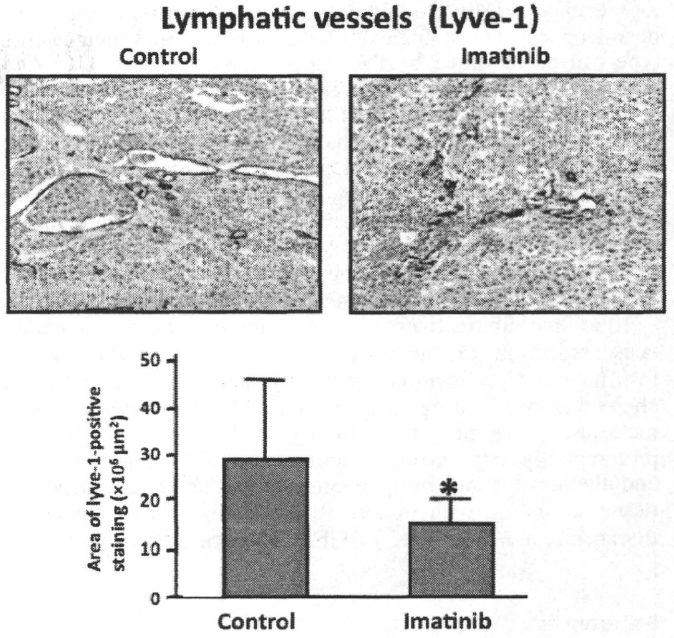

Fig. 4. Immunohistochemistry for Lyve-1 in TMK-1 orthotopic gastric tumors with and without imatinib treatment. Treatment with imatinib significantly reduced the area of lymphatic vessels. *$P < 0.05$; bars, SE.

Discussion

Lymph node metastasis is a common clinical finding in many human cancers and is associated with both aggressive disease and poor prognosis. Genetic and epigenetic alterations of tumor cells often lead to amplified expression of multiple growth factors that contribute to tumor growth, angiogenesis and lymphangiogenesis.[26]

VEGF-C and VEGF-D through interaction with VEGFR-3 expressed on lymphatic endothelial cells were once thought to be the only direct lymphangiogenic factors.[27] However, tumors with high lymphatic metastatic ability express additional growth factors at high levels, suggesting that these factors may contribute to tumor lymphangiogenesis.[26] In an extensive study in which Cao *et al.*[13] implanted PDGF-A and PDGF-B in mouse corneas, both factors were shown to induce growth of lymphatic vessels, although PDGF-B was more potent than PDGF-A. Additionally, its main receptor, PDGF-Rβ, was detected on the induced lymphatic endothelial cells. VEGF-C/-D and VEGFR-3 antagonists did not inhibit PDGF-B-induced lymphangiogenesis. PDGF-B was also shown to activate intracellular signaling components by phosphorylation of Akt, Src, and Erk. In the present study, patients with positive lymph nodes showed significantly greater expression of PDGF-B and PDGF-Rβ than that of node-negative patients.

Tumor blood vessels have been shown to differ morphologically from their normal counterparts. The endothelial cells are structurally and functionally abnormal and can acquire cytogenetic abnormalities while in the tumor microenvironment.[28] Tumor lymphatic vessels appear to be structurally disorganized, tortuous, and leaky.[13] These leaky tumoral lymphatics could provide a vulnerable structural basis for tumor cell invasion into the lymphatic system. Like tumor blood cells, tumor-associated lymphatic vessels have been recently shown to have differentially expressed genes. Clasper *et al.*[29] compared gene expression of purified lymphatic endothelial cells from highly metastatic fibrosarcoma and from dermal tissue. They found differential expression of some 792 genes that code for a variety of proteins including components of endothelial junctions, subendothelial matrix, and vessel growth/patterning. In our orthotopic gastric cancer model, Lyve-1-positive lymphatic vessels were shown to express PDGF-Rβ; not all lymphatic vessels expressed PDGF-Rβ. PDGF-Rβ was expressed occasionally on lymphatic endothelial cells, especially on enlarged and tortuous lymphatic vessels located immediately adjacent to tumor nests, whereas lymphatic vessels in normal tissue or intratumoral small lymphatic vessels did not express PDGF-Rβ. Additionally, we did not find PDGF-Rβ expression on lymphatic vessels of orthotopic tumors grown up from KKLS cells, which express

doi: 10.1111/j.1349-7006.2010.01639.x

low levels of PDGF-B (data not shown). In general, tumor cells in a neoplasm are biologically heterogeneous, and their phenotype can be modified by the organ microenvironment.[30] Our data indicate that tumor-associated lymphatic vessels are also biologically heterogeneous and that interplay between lymphatic vessels and tumor cells may have a more significant effect on the endothelial phenotype than previously anticipated. Additionally, blockade of PDGF-Rβ signaling by oral administration of the PDGF-R tyrosine kinase inhibitor imatinib significantly reduced the area of lymphatic vessels in our orthotopic mouse model of gastric cancer. In our experiment, lymph node metastasis was not inhibited by treatment with imatinib alone (control, 8/10 *vs* imatinib treatment, 7/10). To inhibit lymph node metastasis, reduction of the lymphatic vessel area seems to be insufficient. Combination therapy of imatinib with cytotoxic chemotherapeutic drugs may be needed to inhibit lymph node metastasis. Together, these findings indicate that PDGF-Rβ is preferentially expressed by activated, proliferating lymphatic endothelium but not by quiescent lymphatic vessels in normal tissue, a finding with important implications for the potential therapeutic use of targeted PDGF-Rβ-blocking strategies.

In conclusion, we found PDGF-B secreted by tumor cells and PDGF-Rβ expressed by stromal cells including lymphatic endothelial cells to be associated with lymphatic metastasis in gastric carcinoma. Thus, blockage of PDGF-induced lymphangiogenesis may be a reasonable approach to prevention and treatment of lymphatic metastasis.

Acknowledgments

This work was carried out with the kind cooperation of the Analysis Center of Life Science, Hiroshima University, Hiroshima, Japan, and we thank Novartis Pharma K.K. (Basel, Switzerland) for providing the imatinib used in the study. This work was supported, in part, by Grants-in-Aid for Cancer Research from the Ministry of Education, Culture, Science, Sports and Technology of Japan and from the Ministry of Health, Labor and Welfare of Japan.

Disclosure Statement

The authors have no conflict of interest.

References

1 Fidler IJ. The pathogenesis of cancer metastasis: the 'seed and soil' hypothesis revisited. *Nat Rev Cancer* 2003; **3**: 453–8.
2 Carmeliet P, Jain RK. Angiogenesis in cancer and other diseases. *Nature* 2000; **407**: 249–57.
3 Jussila L, Alitalo K. Vascular growth factors and lymphangiogenesis. *Physiol Rev* 2002; **82**: 673–700.
4 Karkkainen MJ, Haiko P, Sainio K *et al.* Vascular endothelial growth factor C is required for sprouting of the first lymphatic vessels from embryonic veins. *Nat Immunol* 2004; **5**: 74–80.
5 Makinen T, Jussila L, Veikkola T *et al.* Inhibition of lymphangiogenesis with resulting lymphedema in transgenic mice expressing soluble VEGF receptor-3. *Nat Med* 2001; **7**: 199–205.
6 Mandriota SJ, Jussila L, Jeltsch M *et al.* Vascular endothelial growth factor-C-mediated lymphangiogenesis promotes tumor metastasis. *EMBO J* 2001; **20**: 672–82.
7 Skobe M, Hawighorst T, Jackson DG *et al.* Induction of tumor lymphangiogenesis by VEGF-C promotes breast cancer metastasis. *Nat Med* 2001; **7**: 192–8.
8 Stacker SA, Achen MG, Jussila L, Baldwin ME, Alitalo K. Lymphangiogenesis and cancer metastasis. *Nat Rev Cancer* 2002; **2**: 573–83.
9 Kubo H, Cao R, Brakenhielm E, Makinen T, Cao Y, Alitalo K. Blockade of vascular endothelial growth factor receptor-3 signaling inhibits fibroblast growth factor-2-induced lymphangiogenesis in mouse cornea. *Proc Natl Acad Sci U S A* 2002; **99**: 8868–73.
10 Gale NW, Thurston G, Hackett SF *et al.* Angiopoietin-2 is required for postnatal angiogenesis and lymphatic patterning, and only the latter role is rescued by Angiopoietin-1. *Dev Cell* 2002; **3**: 411–23.
11 Kajiya K, Hirakawa S, Ma B, Drinnenberg I, Detmar M. Hepatocyte growth factor promotes lymphatic vessel formation and function. *EMBO J* 2005; **24**: 2885–95.
12 Hirakawa S, Kodama S, Kunstfeld R, Kajiya K, Brown LF, Detmar M. VEGF-A induces tumor and sentinel lymph node lymphangiogenesis and promotes lymphatic metastasis. *J Exp Med* 2005; **201**: 1089–99.
13 Cao R, Bjorndahl MA, Religa P *et al.* PDGF-BB induces intratumoral lymphangiogenesis and promotes lymphatic metastasis. *Cancer Cell* 2004; **6**: 333–45.
14 Pietras K, Sjoblom T, Rubin K, Heldin CH, Ostman A. PDGF receptors as cancer drug targets. *Cancer Cell* 2003; **3**: 439–43.
15 Heldin CH, Eriksson U, Ostman A. New members of the platelet-derived growth factor family of mitogens. *Arch Biochem Biophys* 2002; **398**: 284–90.
16 Li X, Eriksson U. Novel PDGF family members: PDGF-C and PDGF-D. *Cytokine Growth Factor Rev* 2003; **14**: 91–8.
17 Uehara H, Kim SJ, Karashima T *et al.* Effects of blocking platelet-derived growth factor-receptor signaling in a mouse model of experimental prostate cancer bone metastases. *J Natl Cancer Inst* 2003; **95**: 458–70.
18 Risau W, Drexler H, Mironov V *et al.* Platelet-derived growth factor is angiogenic in vivo. *Growth Factors* 1992; **7**: 261–6.
19 Ostman A. PDGF receptors-mediators of autocrine tumor growth and regulators of tumor vasculature and stroma. *Cytokine Growth Factor Rev* 2004; **15**: 275–86.
20 Pietras K. Increasing tumor uptake of anticancer drugs with imatinib. *Semin Oncol* 2004; **31**: 18–23.
21 Japanese Research Society for Gastric Cancer. *Japanese classification of gastric carcinoma*. Tokyo: Kanehara, 1999.
22 Druker BJ, Tamura S, Buchdunger E *et al.* Effects of a selective inhibitor of the Abl tyrosine kinase on the growth of Bcr-Abl positive cells. *Nat Med* 1996; **2**: 561–6.
23 Buchdunger E, Cioffi CL, Law N *et al.* Abl protein-tyrosine kinase inhibitor STI571 inhibits in vitro signal transduction mediated by c-kit and platelet-derived growth factor receptors. *J Pharmacol Exp Ther* 2000; **295**: 139–45.
24 Hwang RF, Yokoi K, Bucana CD *et al.* Inhibition of platelet-derived growth factor receptor phosphorylation by STI571 (Gleevec) reduces growth and metastasis of human pancreatic carcinoma in an orthotopic nude mouse model. *Clin Cancer Res* 2003; **9**: 6534–44.
25 Valencak J, Heere-Ress E, Kopp T, Schoppmann SF, Kittler H, Pehamberger H. Selective immunohistochemical staining shows significant prognostic influence of lymphatic and blood vessels in patients with malignant melanoma. *Eur J Cancer* 2004; **40**: 358–64.
26 Folkman J. Looking for a good endothelial address. *Cancer Cell* 2002; **1**: 113–5.
27 Alitalo K, Carmeliet P. Molecular mechanisms of lymphangiogenesis in health and disease. *Cancer Cell* 2002; **1**: 219–27.
28 Hida K, Hida Y, Amin DN *et al.* Tumor-associated endothelial cells with cytogenetic abnormalities. *Cancer Res* 2004; **64**: 8249–55.
29 Clasper S, Royston D, Baban D *et al.* A novel gene expression profile in lymphatics associated with tumor growth and nodal metastasis. *Cancer Res* 2008; **68**: 7293–303.
30 Fidler IJ, Poste G. The cellular heterogeneity of malignant neoplasms: implications for adjuvant chemotherapy. *Semin Oncol* 1985; **12**: 207–21.

UICC
global cancer control

IJC
International Journal of Cancer

Mesenchymal stem cells enhance growth and metastasis of colon cancer

Kei Shinagawa[1], Yasuhiko Kitadai[1], Miwako Tanaka[1], Tomonori Sumida[1], Michiyo Kodama[1], Yukihito Higashi[2], Shinji Tanaka[3], Wataru Yasui[4] and Kazuaki Chayama[1]

[1] Department of Medicine and Molecular Science, Graduate School of Biomedical Sciences, Hiroshima University, Hiroshima, Japan
[2] Department of Cardiovascular Physiology and Medicine, Graduate School of Biomedical Sciences, Hiroshima University, Hiroshima, Japan
[3] Department of Endoscopy, Hiroshima University Hospital, Hiroshima, Japan
[4] Department of Molecular Pathology, Graduate School of Biomedical Sciences, Hiroshima University, Hiroshima, Japan

Recently, mesenchymal stem cells (MSCs) were reported to migrate to tumor stroma as well as injured tissue. We examined the role of human MSCs in tumor stroma using an orthotopic nude mice model of KM12SM colon cancer. In *in vivo* experiments, systemically injected MSCs migrated to the stroma of orthotopic colon tumors and metastatic liver tumors. Orthotopic transplantation of KM12SM cells mixed with MSCs resulted in greater tumor weight than did transplantation of KM12SM cells alone. The survival rate was significantly lower in the mixed-cell group, and liver metastasis was seen only in this group. Moreover, tumors resulting from transplantation of mixed cells had a significantly higher proliferating cell nuclear antigen labeling index, significantly greater microvessel area and significantly lower apoptotic index. Splenic injection of KM12SM cells mixed with MSCs, in comparison to splenic injection of KM12SM cells alone, resulted in a significantly greater number of liver metastases. MSCs incorporated into the stroma of primary and metastatic tumors expressed α-smooth muscle actin and platelet-derived growth factor receptor-β as carcinoma-associated fibroblast (CAF) markers. In *in vitro* experiments, KM12SM cells recruited MSCs, and MSCs stimulated migration and invasion of tumor cells through the release of soluble factors. Collectively, MSCs migrate and differentiate into CAFs in tumor stroma, and they promote growth and metastasis of colon cancer by enhancing angiogenesis, migration and invasion and by inhibiting apoptosis of tumor cells.

Cancer Cell Biology

Mesenchymal stem cells (MSCs) are characterized by their ability to self-renew and differentiate into tissues of mesodermal origin, including bone, cartilage and adipose and connective tissues. Thus, they contribute to tissue regeneration.[1]

Key words: mesenchymal stem cells, carcinoma-associated fibroblasts, orthotopic colon cancer model, tumor microenvironment

Abbreviations: CAF: carcinoma-associated fibroblast; DAPI: 4′,6-diamidino-2-phenylindole; DMEM: Dulbecco's Modified Eagle's Medium; FACS: fluorescence-activated cell sorting; FAP: fibroblast activation protein; FBS: fetal bovine serum; FSP: fibroblast specific protein; HBSS: Hanks' balanced salt solution; MSC: mesenchymal stem cell; MVA: microvessel area; PBS: phosphate-buffered saline; PCNA: proliferating cell nuclear antigen; PCNA-LI: PCNA labeling index; PDGFR: platelet-derived growth factor receptor; SMA: smooth muscle actin; TUNEL: terminal deoxynucleotide transferase-mediated dUTP-biotin nick end labeling

Grant sponsors: Ministry of Education, Culture, Science, Sports and Technology of Japan (Grants-in-Aid for Cancer Research), Ministry of Health, Labor and Welfare of Japan

DOI: 10.1002/ijc.25440

History: Received 3 Jan 2010; Accepted 28 Apr 2010; Online 6 May 2010

Correspondence to: Yasuhiko Kitadai, Hiroshima University Graduate School of Biomedical Sciences, 1-2-3 Kasumi, Minami-ku, Hiroshima 734-8551, Japan, Tel.: +81-82-257-5191, Fax: +81-82-257-5194, E-mail: kitadai@hiroshima-u.ac.jp

MSCs are recruited from bone marrow to inflamed or damaged tissues by local endocrine signals, resulting in the formation of fibrous scars.[2,3] Tumor tissue contains abundant growth factors, cytokines and matrix-remodeling proteins, explaining why tumors are likened to wounds that never heal.[4] MSCs are reported to migrate to tumor sites as well as sites of injury and to incorporate into tumor stroma, but the effects of interactions between MSCs and tumor cells and the mechanisms underlying these effects remain unclear. Recent coinjection experiments revealed that MSCs promote tumor growth and metastasis.[5–13] Reports suggest that MSCs are involved in tumor invasion and angiogenesis,[5–7,14] immunosuppression[8,9] and inhibition of apoptosis.[11] Mishra *et al.* reported that MSCs can differentiate into carcinoma-associated fibroblast (CAF)-like cells by prolonged exposure to tumor-conditioned medium and that these cells promote tumor growth.[12,13] Theirs was the first report to show the relations between cancer cells, MSCs and CAFs in detail. Because accumulating evidence suggests that CAFs indeed promote the growth of tumors,[15–20] the hypothesis that CAFs originate from MSCs may have interesting clinical implications.

In most coinjection studies concerning the effect of MSCs on tumors, subcutaneous ectopic transplantation models were used, but these models are considered insufficient for examining tumor–stroma interactions.[21] The influence of the organ microenvironment on the biology of tumor cells has been recognized since Paget's "seed and soil" hypothesis,

which suggests that multiple interactions between tumor cells and specific organs determine whether metastasis will occur.[22] Organ-specific factors can influence the growth, vascularization, invasion and metastasis of human neoplasms.[23–25] Thus, we examined tumor–MSC interactions in the tumor microenvironment using a mouse orthotopic transplantation model of human colon cancer.

We found that circulating MSCs migrate not only to the orthotopic colon tumor but also to the metastatic liver tumors. In addition, we showed by coinjection study that MSCs promote the growth and metastasis of colon cancer and that MSCs incorporated into the tumor stroma express CAF markers. This is the first reported study to show the significance of tumor–MSC interactions in the growth and metastasis of colon cancer.

Material and Methods

Isolation and culture of human MSCs

MSCs were obtained from the iliac crest and plated in a dish with Dulbecco's Modified Eagle's Medium (DMEM) supplemented with 10% fetal bovine serum (FBS), L-glutamine and a penicillin–streptomycin mixture according to a protocol approved by the Ethics Committee of Hiroshima University Graduate School of Medicine, as described previously.[26] Nonadherent cells were removed after 72 hr, and adherent cells were detached from the plates and subcultured every 4–5 days in fresh medium supplemented with 1 ng/ml fibroblast growth factor-2.[27] Aliquots from passages 3–5 were frozen in liquid nitrogen for future use.

Characterization of human MSCs *in vitro*

In culture medium, MSCs formed a monolayer of adherent cells and looked like long spindle-shaped fibroblastic cells. The capacity for chondrogenic, adipogenic and osteogenic differentiation was confirmed with the use of a Human Mesenchymal Stem Cell Functional Identification Kit (R&D Systems, Minneapolis, MN). Cell surface antigens on these cells were analyzed by fluorescence-activated cell sorting, and we confirmed that the cells were positive for CD29, CD44, CD73, CD90, CD105, CD166 and MHC-DR, but negative for CD14, CD34 and Flk-1, as described previously.[26]

Colon cancer cell line and culture conditions

The human colon cancer cell line KM12SM[28,29] was kindly gifted by Dr. Isaiah J. Fidler (University of Texas). Cells were maintained in DMEM supplemented with 10% FBS, L-glutamine and a penicillin–streptomycin solution. The cultures were maintained for no longer than 12 weeks after recovery from frozen stock.

Animals and transplantation of tumor cells

Female athymic BALB/c nude mice were obtained from Charles River Japan (Tokyo, Japan). The mice were maintained under specific pathogen-free conditions and used when 8 weeks old. Study was carried out after permission was granted by the Committee on Animal Experimentation of Hiroshima University.

To produce cecal tumors, KM12SM cells in 50 μl of Hanks' balanced salt solution (HBSS) were injected into the cecal wall of nude mice under a dissecting microscope as described previously.[28] To produce experimental liver metastases, the cells were injected into the spleen of nude mice as described previously.[29]

Assessing migration of MSCs *in vivo*

To determine whether circulating MSCs have the ability to migrate to the orthotopic colon tumor, 1.0×10^6 KM12SM cells were transplanted into the cecal wall of three mice on day 0. Three weeks after tumor cell transplantation (on day 21), each mouse underwent injection of 1.0×10^6 PKH26 (Sigma)-labeled MSCs (in 200 μl of HBSS) into the tail vein. One week after this injection (on day 28), the mice were killed and necropsied.

To determine whether circulating MSCs also have the ability to migrate to the metastatic liver tumor, 0.5×10^6 KM12SM cells were transplanted into the spleen of three mice on day 0. One week after tumor cell transplantation (on day 7), each mouse underwent injection of 1.0×10^6 PKH26-labeled MSCs (in 200 μl of HBSS) into the tail vein. Three weeks after this injection (on day 28), the mice were killed.

Tumors were removed and stored in OCT Compound (Sakura Finetek Japan, Tokyo, Japan) and then snap-frozen in liquid nitrogen and stored at −80°C until tissue processing. Sections of PKH26-labeled tissues were analyzed by means of fluorescence confocal microscopy.

Examining the effect of MSCs on tumor growth in orthotopic colon tumors

To examine the effect of MSCs on tumor growth at the orthotopic site, coinjection studies were carried out. Mice were divided into three groups and underwent injection of (a) KM12SM cells alone (0.5×10^6, $n = 24$), (b) KM12SM cells mixed with MSCs [KM12SM:MSCs (0.5×10^6:1.0×10^6, ratio of 1:2, $n = 28$)], or (c) MSCs alone (1.0×10^6, $n = 10$).

Six weeks after intracecal transplantation of these cells, surviving mice were killed and necropsied [(a) $n = 21$, (b) $n = 12$, (c) $n = 10$]. Tumor weights, incidences of liver metastasis, and survival rates were evaluated. One part of the tumor tissue from each mouse was fixed in formalin-free IHC Zinc Fixative (PharMingen, San Diego, CA) and embedded in paraffin, and the other part was embedded in OCT Compound, rapidly frozen in liquid nitrogen and stored at −80°C.

Examining differentiation of MSCs commingled with tumor cells in orthotopic colon tumors

To evaluate whether commingled MSCs can differentiate into CAF-like cells, KM12SM cells mixed with PKH26-labeled MSCs (0.5×10^6:1.0×10^6, ratio of 1:2) were injected into the cecal wall of 3 mice. Three weeks after intracecal

Int. J. Cancer: 127, 2323–2333 (2010) © 2010 UICC

transplantation, tumors were excised. Excised tumors were analyzed by means of fluorescence confocal microscopy to detect PKH26-labeled MSCs after immunofluorescence staining.

Assessing the effect of MSCs on liver metastasis and differentiation of MSCs in a liver metastasis model

To highlight the effect of MSCs on liver metastasis, we developed a model of liver metastasis by injecting tumor cells into mice spleen as described previously.[28,29] Mice were divided into two groups: (a) those injected with KM12SM cells alone (0.5×10^6, $n = 10$), and (b) those injected with KM12SM cells along with PKH26-labeled MSCs [KM12SM:PKH26-labeled MSCs (0.5×10^6:1.0×10^6, ratio of 1:2, $n = 10$)].

Four weeks after intrasplenic transplantation, tumor nodules on the liver surface were counted macroscopically. To examine whether MSCs can migrate from the primary site to the metastatic site and differentiate, metastatic tumors were analyzed by means of fluorescence confocal microscopy to detect PKH26-labeled MSCs after immunofluorescence staining.

Antibodies

The primary antibodies used were rabbit anti-platelet-derived growth factor receptor (PDGFR)-β (Santa Cruz Biotechnology, Santa Cruz, CA), rabbit anti-α-smooth muscle actin (SMA) (Abcam, Cambridge, UK), mouse anti-desmin (Molecular Probes, Eugene, OR), rabbit anti-fibroblast activation protein (FAP) (Abcam, Cambridge, UK), rabbit anti-fibroblast specific protein (FSP) (Abcam, Cambridge, UK), mouse anti- proliferating cell nuclear antigen (PCNA) (Dako, Glostrup, Denmark) and rat anti-mouse CD31 (BD Pharmingen, San Diego, CA). Biotinylated rabbit anti-rat IgG (Dako) and biotinylated goat anti-mouse IgG (Dako) were used as secondary antibodies. The fluorescent secondary antibody was Alexa Fluor® 488-labeled goat anti-rabbit IgG (Invitrogen, Carlsbad, CA).

Immunohistochemical determination of PCNA, apoptotic cells and microvessel area (MVA)

Paraffin-embedded tissues cut into 4-μm sections and frozen tissues cut into 8-μm sections were used for immunohistochemical identification of PCNA and CD31, respectively. Immunohistochemistry was performed as described previously.[30] The PCNA labeling index (PCNA-LI) was expressed as the ratio of positively stained tumor cells to the total tumor cells, given as a percentage for each case. Ten random areas without necrosis in a section were selected by light microscopy; at least 2,000 cells were counted under 400× magnification. Apoptotic cells in frozen sections of KM12SM tumors were detected by terminal deoxynucleotide transferase-mediated dUTP-biotin nick end labeling (TUNEL method) with the ApopTag Plus Peroxidase *In Situ* Apoptosis Detection Kit (Chemicon, Temecula, CA) according to the manufacturer's instructions. The apoptotic index (AI) was expressed as the ratio of positively stained tumor cells and apoptotic bodies to all tumor cells, given as a percentage for each case. Twenty random areas without necrosis in a section were selected by light microscopy; at least 5,000 cells were counted under 400× magnification. Angiogenic activity was evaluated according to the areas of microvessels stained with anti-mouse CD31 antibody. For quantification of the MVA, ten random fields at 100× magnification were captured for each tumor, and the outline of each microvessel including a lumen was manually traced. The area was then calculated with the use of NIH ImageJ software.

Immunofluorescence staining

Frozen specimens cut into 8-μm sections or cells cultured on slide glass were fixed for 15 min in 4% paraformaldehyde in phosphate-buffered saline (PBS). The slides were blocked briefly in protein blocking solution, incubated overnight at 4°C with the Fab fragment of anti-mouse IgG to block endogenous immunoglobulins if necessary, and incubated overnight at 4°C with anti-α-SMA (1:400), anti-FAP (1:100), anti-FSP (1:100), anti-desmin (1:400) or anti-PDGFR-β (1:400). The slides were washed with PBS and then incubated for 1 hr at room temperature with Alexa Fluor® 488-labeled secondary antibody (1:600). Nuclear counterstain with 4′,6-diamidino-2-phenylindole (DAPI) was applied for 10 min, and mounting medium was placed on each specimen with a glass coverslip. α-SMA-, FAP-, FSP-, desmin- or PDGFR-β-positive cells were identified by green fluorescence, whereas PKH26 on MSCs was identified by red fluorescence. Colocalization of PKH26 and α-SMA, FAP, FSP, desmin or PDGFR-β was detected by yellow staining.

Confocal microscopy

Confocal fluorescence images were captured with a 20× or 40× objective lens on a Zeiss LSM 510 laser scanning microscopy system (Carl Zeiss, Thornwood, NY) equipped with a motorized Axioplan microscope, argon laser (458/477/488/514 nm, 30 mW), HeNe laser (543 nm, 1 mW), HeNe laser (633 nm, 5 mW), LSM 510 control and image acquisition software and appropriate filters (Chroma Technology Corp., Brattleboro, VT). Confocal images were exported to Adobe Photoshop software, and image montages were prepared.

Collection of conditioned medium

To detect any paracrine effects of MSCs on KM12SM cells, conditioned medium from MSCs was collected and used for subsequent study. In detail, 1.0×10^6 MSCs were seeded in a 100-mm plate, and 48 hr later, 20 ml of DMEM with 0.5% FBS was added for 24-hr incubation. The medium was then collected, sterile filtered, aliquoted and stored at −20°C until use. DMEM with 0.5% FBS was used as control medium.

Proliferation assay

The proliferative effect of MSC-conditioned medium on KM12SM cells was analyzed. KM12SM (4.0×10^4) cells were